AD-A108 476 SCIENCE APPLICATIONS INC MCLEAN VA F/G 17/1

IMPROVED APPROACH FOR MODELING ACOUSTIC FLUCTUATIONS.(U)

OCT 79 R C CAVANAGH, W W RENNER N00014-78-C-0603

UNCLASSIFIED SAI-80-104-WA NL

CONT

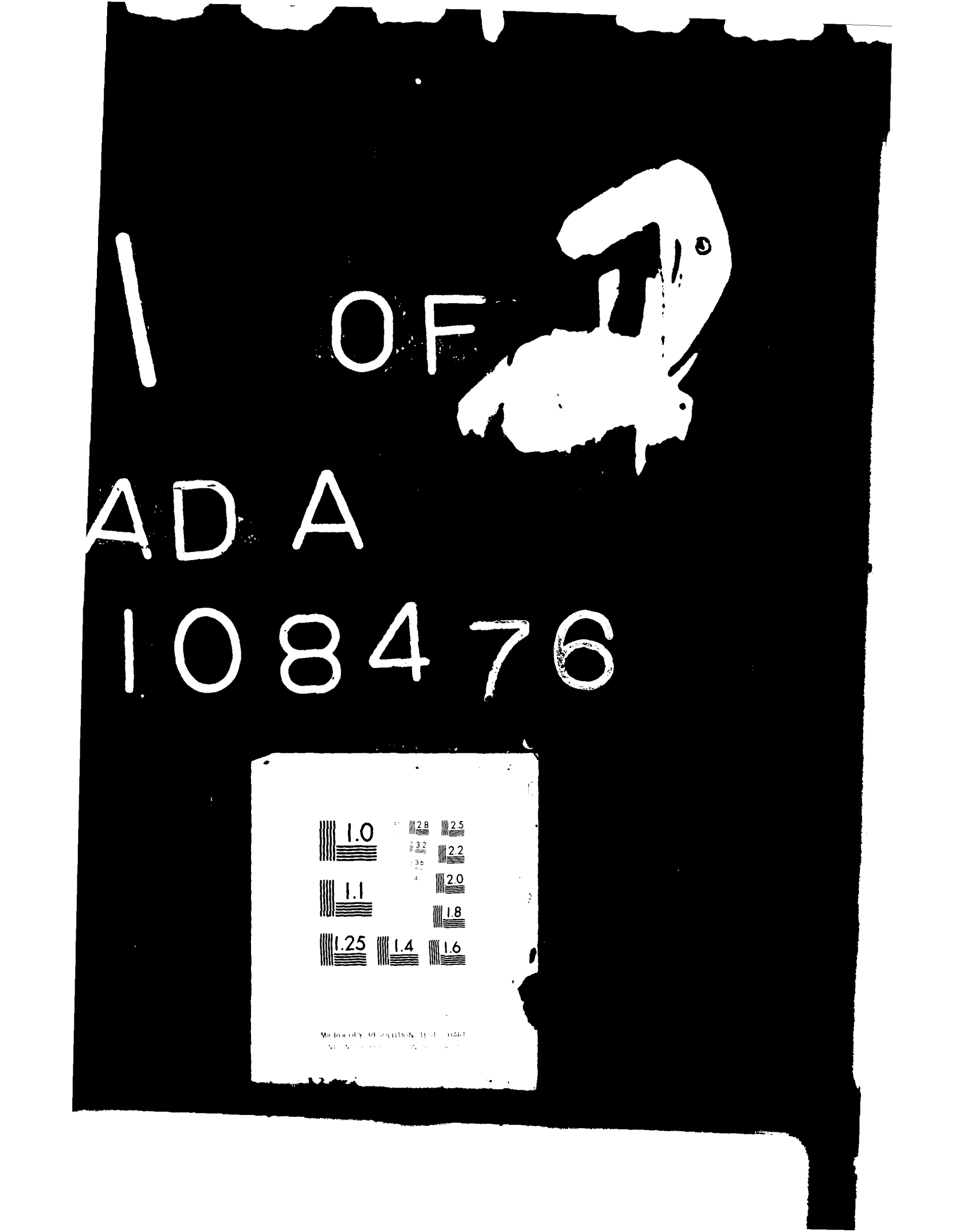
1 OF 7
AD A
108476
1.0
1.1
1.25
1.4
1.6
2.8
3.2
3.6
2.5
2.2
2.0
1.8

LEVEL II

IMPROVED APPROACH FOR MODELING ACOUSTIC FLUCTUATIONS

ATLANTA • ANN ARBOR • BOSTON • CHICAGO • CLEVELAND • DENVER • HUNTSVILLE • LA JOLLA
LITTLE ROCK • LOS ANGELES • SAN FRANCISCO • SANTA BARBARA • TUCSON • WASHINGTON

IMPROVED APPROACH FOR MODELING ACOUSTIC FLUCTUATIONS

SAI Report 80-104-WA

Final Report
Contract N00014-78-C-0603
Task Number NR ...

October 1979

Prepared by:

R.C. Cavanagh
W.W. Renner
Ocean Science Division

Prepared for:

Office of Naval Research
Naval Analysis Program
Code 431
Mr. J.G. Smith

SCIENCE APPLICATIONS, INC.
8400 Westpark Drive
McLean, Virginia 22102
(703) 821-4300

CONTENTS

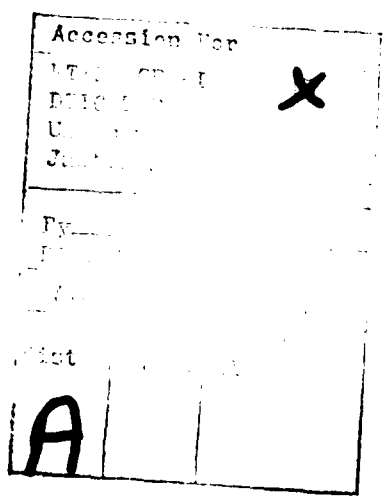

Section 1
INTRODUCTION

The Navy relies on sonar-system performance predictions for many applications -- from concept and design through direct Fleet tactical aids. Each application involves a specific amount of ensembling over conditions and requires a certain level of accuracy. Performance predictions are usually generated through detection or tracking simulations, employing computer models for engagements between targets and sensors. Whether a Monte Carlo or analytic approach is used, the statistical results depend principally on the scenario, the system response and the acoustic environment. This study concentrates on the last item, the environmental acoustic (EVA) parameters and their fluctuations, and how it impacts performance-prediction capability.

A substantial amount of Navy R&D effort has been concerned with understanding and modeling the averaged and detailed properties of EVA parameters (specifically, sound transmission, ambient noise, and reverberation). The critical questions related to this work are:

(a) Under given ensembling conditions (application), how sensitive are performance model predictions to the EVA inputs?

(b) What is the level of accuracy (detail) needed in the estimation of EVA data as a function of the type of ensembling?

(c) Given answers to (a) and (b), how should the EVA properties and system performance be estimated?

(d) In particular, are there efficient means for calculating measures of effectiveness, detection statistics, and detailed properties of the EVA parameters?

The four questions are non-trivial and cannot be resolved completely in this investigation (see, e.g., Reference 1-1 for a sample of recent research and evidence that the acoustic community is not ready to address the problem). The present effort does, however, consider important parts of each question. The work has proceeded in two phases, as described next.

The first phase (Ref. 1-2) concentrated on low-frequency, passive sonar and questions (c) and (d); that the Navy had developed and was using performance prediction models based on a specific approach: random-process simulations for acoustic or system fluctuations and Monte-Carlo calculations of MOE's (detection probabilities, holding times). It was determined that the accuracy of the random-process approach was strongly dependent on the use of accurate input parameters:

- Mean Transmission Loss at Array Output (TL).
- Mean Noise at Array Output (Beam Noise).
- Distributions and Temporal-Correlation Properties of TL and Beam-Noise Fluctuations.

It was further concluded that the random-process approach could be improved by (i) the selection of random-process models with properties more like those of actual acoustic fluctuations, and by (ii) more efficient means for determining the EVA statistical inputs, such as those listed above.

The second and current phase of investigation has two concerns:

I. Initial consideration of questions (a) and (b), especially as related to calculating a specific MOE: cumulative detection probability ($CP/_D$).

II. Improvement of the random-process approach in response to the recommendations just mentioned (i & ii).

For item I, the first priority was to gain an understanding of the sensitivity of performance predictions to the accuracy of EVA inputs for various levels of ensembling (over target tracks, diurnal variations, etc.). A special case in which a signal-to-noise-ratio (SNR) detector operates against deterministic SNR was used to study the ensembling question in great detail. Deterministic and various types of random tracks were considered. The results showed sensitivity of discrete and cumulative detection probabilities (P_D and CP_D) to ensembling, and were then extrapolated to more general cases. Although the solution is not complete (this was an initial and limited effort),

the illustrations of Section 2 should be of considerable value to performance modelers for determining input-accuracy requirements and for interpreting their predictions.

The second problem pursued under item I is that of practically estimating CP_D for "realistic" acoustic environments. Most detection simulations (see again Reference 1-20 employ random-process models for signal and noise fluctuation with special forms (e.g., exponential autocorrelations) which generally do not yield faithful facsimiles of the usual quasi-periodic variations. Moreover, there seems to be some confusion about the underlying properties of signals and noise, and how they impact instantaneous detections (e.g. via ROC curves), and how they affect overall system performance (e.g. CP_D). Section 3 documents an initial effort to address these problems, first by carefully describing the detection problem in terms of basic signal and noise properties, and then by deriving an approach for calculating CP_D for a "realistic" fluctuating signal-to-noise ratio (SNR). Again, the results should be valuable to performance models, both as aids to interpreting their results and as improvements to modeling methods.

Turn now to the second item (II) of interest here: improvement of the currently popular random-process approach for fluctuation modeling in performance analyses. The effort (just described) to use realistic SNR for CP_D calculations represents a contribution in Problem Area II. However, additional work concentrated on approaches for obtaining the key features of TL and noise fluctuations without the extensive computer computations usually required.

Section 4 and a comparison report attack the TL fluctuation problem. The premise is that fluctuations in transmission for most passive sonar applications are caused by relative source/receiver motion.

A separate document (Ref 1-3) provides a solution to a problem of great interest in the EVA community--how to efficiently model TL for a moving source. The conclusion is that, under reasonable conditions, variations in multipath interference induced by source/receiver motion can be accurately modeled with ray or wave theory in a "frozen" ocean. It is not necessary to integrate the time-dependent wave equation. The resulting shortcut is of considerable importance, and the analysis is summarized in this document.

With the cause of the TL fluctuations and an approach to model them identified, an efficient ray-theoretic method has been developed to provide the important spatial properties of the TL fluctuations, which in turn are converted to temporal properties for dynamic scenarios. The technique required a very modest amount of ray-tracing and has been applied to both bottom and waterborne paths. The computer program and associated graphics package have been used in Section 4 to test the results against detailed TL model predictions and to investigate the sensitivity of the fluctuation statistics to the environmental inputs. It is expected that the algorithm will find extensive applications in providing inputs to performance models.

Just as for TL, a short-cut for predicting key features of beam-noise fluctuations at low frequency (ship-generated noise) would be a valuable asset for performance-

prediction applications. The various noise fluctuation schemes in current use were reviewed in detail (from Reference 1-4). Limitations in the most promising candidates were identified, and a variation of an existing technique selected. Results were tested against "Brute Force" simulations. The investigation is documented in Section 5.

Finally, given TL and noise fluctuation properties, the remaining problem under item II is to identify random-process models which more closely reflect those properties than currently popular processes (e.g., Jump, Gauss-Markov, Ehrenfest). Section 6 recommends certain auto-regressive schemes as candidate fluctuation processes.

In summary, this study has considered a variety of questions related to sonar performance modeling. Progress has been made in describing the general sensitivity and approach for calculating CP_D as well as in developing methods for generating EVA inputs to detection and tracking simulations.

Section 2
DETECTION PROBABILITIES FOR A REALISTIC ACOUSTIC ENVIRONMENT

2.1 Introduction

Sonar system performance is traditionally gauged in terms of instantaneous detection and false-alarm probabilities (P_D and P_{FA}). Among the most important measures of effectiveness for both surveillance and tactical ASW systems is the long-term, accumulated effects of numerous detection opportunities: the cumulative detection probability (CP_D).

Efforts to understand and model CP_D in the past have been principally focused on two approaches: the independent glimpse model and random-process simulations. In the first, the detection opportunities are assumed to become statistically independent after some waiting time, so that CP_D is a simple function of individual P_D's. The second is concerned with the acoustic signal and noise, treating each (or their ratio) as structured random processes (e.g., Markov, with Gaussian marginal densities). Detections then occur whenever thresholds are exceeded. In both cases it has been standard procedure to model the acoustic signal and noise as very smooth functions (of time or range) to which are added random fluctuations.

Seldom are the underlying structures of the signal and noise and their relationship with the instantaneous and cumulative detection process properly defined. Concepts of

independence, decorrelation, and P_D itself are often confused, especially when there is ensembling over target or other conditions. Subsection 2.2 proposes a unified view of the acoustic detection problem, including the detector and fluctuations.

Note next that research in environmental acoustics over the past several years has led to a new understanding of the temporal and spatial variations of both signals and ambient noise. In particular, it is usually the case that the fluctuations are quasi-periodic, with predictable periods and amplitude statistics, and that there are statistically well-defined states of slowly varying, smooth, mean values. Part of the present investigation endeavors to develop algorithms for efficiently predicting these important features of the acoustic environment (see Sections 4 and 5). This section deals with the problem of calculating CP_D from such a description - extending the "glimpse" and "random-process" approaches to the more complex and structured signal and noise fields.

Subsection 2.3 defines the general CP_D problem, given the underlying structure. Traditional characterizations of the signal and noise, and approaches to CP_D calculations are summarized in Subsection 2.4. Finally, a "realistic" model of the acoustic variables and a means to obtain the attendant CP_D are presented in the final section.

2.2 Underlying Structure for Detection Process

A review of the standard references for acoustic detection suggests two levels of detail. From a signal-processor's point of view (e.g. Reference 2-1 or 2-2), estimates of signal-plus-noise and noise are somehow manipulated (filtered, integrated) and compared, with detection called according to a preselected rule (threshold). The input variables are modeled as random processes and both correct detections and false alarms are possible (with probabilities P_D and P_{FA}). It is standard practice to treat one detection opportunity (integration period) at a time, and to ignore the concept of CP_D. On the other hand, sonar performance and engagement modelers (see, e.g., References 2-3 and 2-4) tend to assume a binary detector operating on the random process SE(t), usually the integrated signal excess estimated from the signal-processor's output. A correct detection occurs when SE(t)>0 and does not otherwise. P_D is then the probability that SE>0, and the false alarm rate is not explicitly given. Cumulative probability (CP_D) is then the chance that SE(t)>0 for some t in an extended time interval.

The two views are not very consistent, and, although cases can be fabricated to bring them into agreement, serious complications arise when the signal-processor's detector and the engagement-modeler's random process must be incorporated in a careful calculation of CP_D. How does decorrelation time fit in? What are independent, the detection events or the random-process samples?

To properly treat the CP_D problem a scheme for viewing the detection process is proposed next, with the intent of including the two viewpoints discussed above.

First, let X and Y be vector-valued variables which represent, respectively, the received signal and noise fields, and the detection rule for a predetermined detection-opportunity interval. Then, in general, detection probability (P_D) is the probability that X and Y take on certain values; P_{FA} has a similar definition. This almost trivial structure is intended to include nearly any signal processor scheme.

The complicating and crucial second step is to force the dependence of P_D and P_{FA} on X and Y in a special form:

> Assume the existence of a summary description (statistic), SN, for X and Y at each time interval such that P_D and P_{FA} depend only on that description. In other words detections and false alarms occur according to values assumed by SN at each opportunity.

This is the usual approach for construction of an ROC curve, with SN some averaged signal-to-noise ratio.

Next, if SN is deterministic (as is usually the case for signal processor's ROC curves), then P_D and P_{FA} are real numbers. If, however, SN is a <u>random variable</u>, then so are P_D and P_{FA}; this is the point at which confusion can begin. Return to the original definition of P_D, where the

implication is that the probability is based on the population X and Y. It follows that if SN must be modeled as a random variable to include the effect of those populations, then the correct value of P_D will be obtained only as an ensemble over the population of SN. Such ensembling takes the form of an expected value over the possible values (Z) of SN:

$$P_D(\{SN\}) = \langle P_D(SN|SN=z)\rangle_z \qquad (2\text{-}1)$$

This type of expression is generally true for any random variable, e.g., in terms of the mean value, $\bar{W}$, of variable W,

$$\underline{P}(W>C)$$

$$= \quad P(W>C|\bar{W}=x)\ P(\bar{W}=x)\ dx$$

$$= \quad E_{\bar{W}}(P(W>C|W)) \qquad (2\text{-}2)$$

Continue now with the concept of cumulative detection probability ($CP_D(T)$: the probability that over a fixed time interval (say [0,T], including a number of detection-opportunity periods) there is at least one detection. For the first definition of P_D, it is the probability of X and Y assuming certain values over at least one detection period. Likewise for SN_i or $SN(\ _i)$, the values of SN at the i-th opportunity interval $\ _i$.

- If SN_i are deterministic, then so are the associated detection probabilities, P_{D_i}. Moreover, it is usual to presume that P_{D_i} depends only on SN_i, and not on any previous or future values of SN. In that case,

$$CP_D(T) = 1 - \prod_i (1-P_{D_i}) \qquad (2\text{-}3)$$

the usual form of CP_D for "independent" detection opportunities.

- If SN_i are random variables, then so are the P_{D_i}. If the variables are independent, then

$$CP_D(T) \quad 1 - \Pi\,(1-E(P_{D_i}))$$

(i.e., we have ensembled over all values of (SN_1, SN_2,...)).

- If the SN_i are random, but not necessarily independent, then $CP_D(T)$ is non-trivial, and no general formula can be given without additional assumptions about SN_i .

Subsequent subsections are concerned with the latter problem.

2.3 The CP_D Problem

The aim here is to investigate cumulative detection probability (CP_D) defined as

$$CP_D(T) = \text{Probability } \{\text{Detection Occurs at Least Once in the Time Travel } [0,T]\}$$

It will be convenient to use the complement:

$$Q(T) = 1 - CP_D(T) = \text{Probability } \{\text{No Detection in } [0,T]\}.$$

To make the notation somewhat more precise, define the following events.

$A(t)$ = Event that detection occurs at time t,

$A(t,\tau)$ = Event that detection occurs at least once in time interval $(t,\ t+\tau)$,

$A[t,\tau]$ = ---------- $[t,\ t+\tau]$,

$\tilde{A}(t)$ and $\tilde{A}(t,\tau)$: events complementary to $A(t)$ and $A(t,\tau)$.

Then

$$P_D(t) = P(A(t)),$$

$$CP_D(t) = P(A[0,t]),$$

$$Q(t) = P(\tilde{A}[0,t]).$$

It is common practice to calculate CP_D stepwise from the general recursive relationship:

$$Q(T + \Delta t) = Q(T) \cdot (1 - P(T;\Delta t)), \qquad (2\text{-}4)$$

or

$$CP_D(T + \Delta t) = 1 - (1 - CP_D(T))\,(1 - P(T;\Delta t)), \qquad (2\text{-}4')$$

$$= CP_D(T) + P(T;\Delta t)\,(1 - CP_D(T))$$

where

$P(T;\Delta t) \equiv$ Probability that detection occurs in the interval $(T, T + \Delta t]$, given that no detection has occurred in $[0,T]$

$$= P(A(T,\Delta T] \mid \tilde{A}[0,T]). \qquad (2\text{-}5)$$

Equation (2-4) is then no more than the definition of the conditional probability. When $Q(t) = 0$, $P(t;\Delta t)$ is undefined, but may be arbitrarily set to 0 or 1 or whatever. If the underlying process is Markov, then $\tilde{A}[0,T]$ can be replaced by $\tilde{A}(t)$ for any t in $[0,T]$.

If we consider discrete time steps $0, \Delta t, 2\Delta t, \ldots, N\Delta t = T$, then

$$Q_{N+1} \equiv Q((N+1)\Delta t) = Q(N\Delta t) \cdot (1 - P(N\Delta t;\Delta t))$$

$$= Q_N \cdot (1 - P(N\Delta t;\Delta t))$$

$$= \ldots = \left(\prod_{j=1}^{N}(1 - P(j\Delta t;\Delta t))\right) \cdot Q_1 \qquad (2\text{-}6)$$

where $1-Q_1$ is the "initial" probability of detection over $[0, \Delta t]$.

If the process is treated as continuous in t, then the existence of the limit

$$\lim_{\Delta t \to 0} \left(\frac{P(t;\Delta t)}{\Delta t} \right) = \hat{p}(t) \tag{2-7}$$

implies that

$$Q'(t) = \lim_{\Delta t \to 0} \left(\frac{Q(t+\Delta t) - Q(t)}{\Delta t} \right)$$

$$= -Q(t) \cdot \hat{p}(t). \tag{2-8}$$

Then

$$Q(T) = Q(0) \cdot \exp \left(- \int_0^T \hat{p}(t)dt \right), \tag{2-9}$$

or

$$CP_D(T) = 1 - (1 - CP_D(0)) \exp \left(- \int_0^T \hat{p}(t)dt \right). \tag{2-9'}$$

In some cases (2-9) is preferred to (2-6); however (2-7) may not exist and the integration time, Δt, is usually finite.

Whichever applies, discrete or continuous time steps, the problem is to calculate $P(t;\Delta t)$ of (2-5). The remainder of this section is concerned with models of SN(t), the detection process, and the calculation of CP_D using (2-5).

2.4 Examples and Traditional Approaches

This section considers progressively more difficult problems, with popular models of SN(t) and the detection process. It leads toward a realistic model for the case of interest, to be attacked in the next section.

2.4.1 Problem 1

$$\left\{\begin{array}{l} SN(t) \text{ is a deterministic function of } t. \\ P_D(t) \equiv P(SN(t) \geq L) \text{ for some fixed } L. \\ P_{FA}(t) \equiv 0 \end{array}\right\}$$

Then

$$P_D(t) = \begin{cases} 0 \text{ if } SN(t) < L \\ 1 \text{ if } SN(t) \geq L \end{cases}$$

$$CP_D(T) = \begin{cases} 0 \text{ if } SN(t) \text{ never exceeds } L \text{ for } 0 \leq t \leq T \\ 1 \text{ otherwise} \end{cases}$$

$$= \max_{0 \leq t \leq T} \{P_D(t)\} .$$

Note that P_D and CP_D are completely deterministic. There is no "accumulation of independent opportunities," and CP_D is just the largest P_D.

Example Problem 1 is so simple that the use of (2-9) or (2-6) is not required.

2.4.2 Problem 2

$$\begin{cases} SN(t) \text{ is a deterministic function of } t. \\ P_D(t) = G(SN(t)) \text{ is a deterministic function, but not limited to values } \{0,1\}. \\ P_{FA}(t) \text{ is similarly defined [say, } H(SN(t))]. \end{cases}$$

Although it appears only superficially more general than Problem 1, this case encompasses many of the difficulties associated with defining and calculating CP_D. It is commonly encountered, with the most typical example being that in which the detector performance is defined by an ROC function, so that P_D depends on short-term, averaged, output statistics of signal-plus-noise and noise (called "SN(t)" here).

It must be emphasized at the outset that SN(t) is a deterministic function. Hence, all uncertainty in the detection process is reflected in the function G which maps the real number SN into a detection probability. To this point, there is no concern about any underlying signal or noise or processing or threshold; it is all contained in G (and the P_{FA} function). However, as we proceed to the calculation of CP_D, notice that the lack of a better description of SN and P_D causes difficulties.

At each point or interval in time (discrete or continuous) there is an opportunity to detect quantified by the instantaneous and deterministic $P_D(t)$. This is not enough information, however, to calculate CP_D. In particular, the dependence of the detection events from one time step to the next is required.

In terms of detection events, we know

$$P_D(t) = P(A(t)) \text{ or } P_D(t) = P(A(t,\Delta t]),$$

$$CP_D(T) = P(A[o,T]).$$

If the events $A[o,\Delta t]$, $A(\Delta t, 2\Delta t],\ldots,A(N\Delta t,(N+1)\Delta t]$ were mutually independent, then

$$P(k\Delta t;\Delta t) = P(A(k\Delta t,\Delta t]|A[o,k\Delta t])$$

$$= P(A(k\Delta t,\Delta t])$$

and from (2-6),

$$CP_D\ (N+1)\Delta t) = 1-\left(\Pi(1-P(j\Delta t;\Delta t))\right)(1-P(A[o,\Delta t]$$

$$= 1 - \left\{\prod_{j=1}^{N}(1-P(A(j\Delta t,\Delta t]))\right\}(1-P(A[o,\Delta t])). \tag{2-10}$$

This is the "independent glimpse" result, so often applied in surveillance. If on the other hand, all of the cited events were totally dependent, then

$$P(k\Delta t;\Delta t) = P(A(k\Delta t,\Delta t]\,|\,\tilde{A}[o,k\Delta t])$$

$$= 0, \text{ for all } k,$$

and again from (2-6),

$$CP_D((N+1)\Delta t) = P\big(A[o,\Delta t]\big) = P\big(A(j\Delta t,\Delta t]\big), \text{ for all } j. \tag{2-11}$$

For a continuum of time steps, the events A(t) are of interest. For the case of independence among all events, the existence of p from (2-4),

$$\hat{p}(t) = \lim_{\Delta t \to o} \left(\frac{P(A(t;\Delta t))}{\Delta t} \right),$$

gives the result analogous to (2-10), from (2-9'):

$$CP_D(T) = 1-(1-CP_D(0))\exp\Big(- \int_0^T \hat{p}\,(t)dt\Big). \tag{2-12}$$

For totally dependent events, $\hat{p} = 0$, and

$$CP_D(T) = CP_D(0). \tag{2-13}$$

These special cases should illustrate the importance of defining the degree of dependence among the events A. This goes far beyond the specification of instantaneous P_D's. Finally, note that P_D and CP_D are real numbers, not random variables. We hear too often in the context of this problem the meaningless statement that the P_D's are independent or dependent.

2.4.3 Problem 3

$$\begin{cases} SN(t) \text{ is a random process} \\ P_D(t) = P(SN(t) \geqslant L), \text{ for fixed threshold } L \\ P_{FA} \text{ is fixed, independent of SN} \end{cases}$$

This is perhaps the model most often used in ASW detection problems. It is like Problem 1 in that the detector is easily defined as a thresholding process; however, the quantity tested is no longer deterministic, but rather a random variable at each time step. In Problem 2, the uncertainty was concentrated in the detection process; here it is contained in the underlying input to the detector (the detector behaves deterministically). The level-crossing properties of the random process SN(t) are what determine P_D and CP_D.

As an aside, we note that confusion can arise when the deterministic SN(t) of Problem 1 is complicated, and is thus replaced with a simpler random process which is supposed to incorporate the important statistical features of SN. The trouble is that such descriptors as decorrelation time or

one-dimensional moments which fully determine the random process may not be appropriate for the deterministic time series (e.g., a nearly sinusoidal signal).

Substantial efforts have been devoted over the past ten years to the calculation of CP_D (and other MOE's) for a class of random processes, especially Gauss-Markov, Jump, and related variations (Ref. 2-5 to 2-7). When the random process represents the fluctuation term, it is added to a deterministic term (e.g., the smooth signal), and the level-crossing CP_D problem is non-trivial. A recursive solution for the Jump process is available (Ref. 2-7), but no such general result is known for the Gauss-Markov or others. Since analytic solutions are rare, it is common practice to employ Monte Carlo simulations in the search for CP_D.

Example To illustrate the complexity of this problem, consider first the simplest "constant-threshold" case for the Gauss-Jump process. Let $SN(t)=X(t)$ be a zero-mean Jump (λ,σ) process (Ref. 2-7), and let detection occur when $SN(t) \geq o$. Then

$$CP_D(T) = P(X(t)>o \text{ for some } t\in [o,T])$$

$$= 1 - P(X(t)<o \text{ for all } t)$$

$$= 1 - \left\{\sum_k P(X(t)<o \,|\, k \text{ jumps}) \cdot P(k \text{ jumps})\right\}$$

$$= 1 - (1-Po)e^{-\lambda TPo}, \qquad (2\text{-}14)$$

where $Po = P(X(t)>o)$ for fixed t. In terms of (2-5)

$$P(t;\Delta t) = 1-e^{-\lambda \Delta t Po}, \qquad (2\text{-}15)$$

and $$\lim_{\Delta t \to o} \frac{P(t;\Delta t)}{\Delta t} = \hat{p}(t) = \lambda Po. \qquad (2\text{-}16)$$

Hence (2-9') yields (2-14).

However, if SN(t) is modeled as

$$SN(t) = L(t) + X(t)$$

where X(t) is as above and L(t) is deterministic, the problem becomes substantially more difficult. For the simplest case of L(t) monotone decreasing, and with

$$P(t) = P_D(t),$$
$$\hat{p}(t) = \lambda P(t) - (P'(t)/(1-P(t). \qquad (2\text{-}17)$$

Hence, $$CP_D(t) = 1 - (1-P(t))\exp\left(-\lambda \int_o^t P(\tau)d\tau\right). \qquad (2\text{-}18)$$

When L(t) is oscillatory, endpoint conditions must be matched with a recursive scheme.

2.4.4 Problem 4

SN(t) is a random process

$P_D(t) = G(SN(t))$

$P_{FA}(t)$

} as in Problem 2, and deterministic

This problem includes all of the complications of Problems 2 and 3: uncertainties in detectability are the result of random acoustic parameters (embodied in SN(t)) and a random dectection process (represented by G). It is the most realistic model of those presented so far since the detector is in practice (and in most performance estimates) not a deterministic thresholder and since the acoustic signal and noise are best seen as random fluctuations added to deterministic functions.

Careful interpretation of P_D and CP_D is required. G is meant to map the random variable SN(t) into a single P_D; it is not intended that P_D be random. Hence G(SN(t)) could be $P(SN(t) \geq L)$ as in Problem 3, or some other ensemble probability. Likewise, CP_D should be an ensemble function of the random process SN(t) and not a random process itself.

Mathematical approaches to calculating CP_D must employ the underlying detection-event structure introduced in Problem 2. Thus, as in that case, more information about dependence than is stated above is required. This might be made clearer if P_D is viewed as follows (see Subsection 2.2):

$$P_D(t) = \int P(\text{Detection} \mid SN(t)=x) \cdot p(SN(t)=x)\, dx$$

$$= E\left\{P(\text{Detection} \mid SN(t))\right\}. \qquad (2\text{-}19)$$

Similar expressions for $P(t;\Delta t)$ and $CP_D(t)$ suggest that these probabilities can be treated as expectations, over the random process (SN(t)), of conditional detection probabilities. The conditionals in turn can be known only when the underlying dependence among detection events is specified.

It should suffice to say, without examples, that Problem 4 is difficult to solve analytically. It does foreshadow the realistic model presented in the next section.

Table 2-1 displays the salient features of each of the four problems treated here.

2.5 CP_D for a Realistic Acoustic/Detector Model

2.5.1 Acoustic Variables

We concentrate on passive sonar applications. A rather general formulation for most cases of interest is as follows:

- Detector performance at discrete time step t_i depends on an integrated variable, $SN(t_i)$, at the output of the beamformer/processor system.

- There are a number of States or conditions which strongly influence the behavior of SN. The chances of a state obtaining and the time in state, etc. are described by a stochastic process or by a deterministic specification.

- Whenever a single state applies for a number of time steps, SN(t) has significant structure. This structure is well-described by periodicity (or quasi-periodicity) of sinusoid-like time series with a distribution of peak amplitudes.

Problem	SN(t)	$P_D(t)$	$P_{FA}(t)$	$CP_D(t)$
1	Deterministic	P(SN(t)>L)	0	$\max_t P_D(t)$
2	Deterministic	G(SN(t)), Deterministic	H(SN(t))	Depends on dependence of "detection events"
3	Random Process	P(SN(t)>L)	Fixed	Found from level-crossing properties of SN(t)
4	Random Process	G(SN(t)), Deterministic	H(SN(t))	Depends on both dependence of "detection events" and properties of random process SN(t)

TABLE 2-1

All of this is suggested by the structure of acoustic signal-to-noise ratio in which the principal fluctuations are exhibits of regular multipath interference patterns and the states are such conditions as: CZ propagation, BB propagation, beam-free noise, beam-occupied noise, and combinations thereof. Sections 4 and 5 of this report discuss the signal and noise properties in some detail.

2.5.2 Special Problems

As in Subsection 2.4, we will attack the CP_D problem in steps of increasing difficulty, beginning with a deterministic SN(t) and threshold detector and finishing with the most general case. As the results are obtained, the effect of added complexities and randomness will be studied - so that efficient algorithms can be developed at appropriate levels of detail.

Problem A

$$\left\{\begin{array}{l} \text{SN(t) deterministic} \\ \\ P_D = P(SN(t) \geq L). \\ \\ P_{FA} = 0 \end{array}\right\}$$

Just as for Problem 1, $CP_D(T) = \max_{0 \leq t \leq T} \{P_D(t)\}$, and hence either 0 or 1 depending on whether SN(t) ever exceeds L. When SN(t) is a quasi-sinusoid in each state, we need only find the highest "peak" in each state, and then the greatest of these. The problem is trivial, and in fact solutions are given in the next section in the study of sensitivity.

Problem B

$$\left\{\begin{array}{l} \text{SN(t) deterministic, quasi-sinusoid} \\ \qquad \text{for each of several states} \end{array}\right\}$$

$$\left\{P_D = G(SN), \text{ deterministic}\right\}$$

$$\left\{P_{FA} = H(SN)\right\}$$

Just as for Problem 2, some statement must be made about the dependence of detection events. Suppose first that they are all independent, then correlated. This problem is nearly equivalent then to A, and the approach the same as that described in Section 3.

Problem C

$$\left\{\begin{array}{l} \text{SN(t) a random process within each} \\ \qquad \text{state; states deterministic} \end{array}\right\}$$

$$\left\{P_D = P(SN \geqslant L)\right\}$$

$$\left\{P_{FA} \text{ fixed}\right\}$$

This is a difficult problem, but a solution has been found for a realistic special case. SN(t) is presumed to consist of a deterministic sinusoid modulated by a jump process. The recursive scheme of Ref. 2-7 has been applied, and the resulting algorithm tested.

Section 3

SENSITIVITY OF PERFORMANCE PREDICTIONS TO ENSEMBLING

In the previous section, great care was taken to define the underlying signal and noise processes and their implications for P_D and CP_D calculations. Even for the case of a stable source, single source/receiver geometry, and fixed system response the analysis can be quite complex, requiring ensemble averaging over fluctuating parameters and non-trivial accumulation of instantaneous detection probabilities. Nonetheless, this "deterministic" scenario can be important for some applications (e.g., reconstruction of a controlled experiment or explanation of a detection event with known target), and the sensitivity of the performance model outputs to the details of the EVA-parameter inputs is relatively well understood. Turn then to other common applications in which the single, "deterministic" event is only one replication of many.

It is the rule in engagement modeling, and often the case in performance analyses, that predictions or simulations are generated for a number of conditions and displayed as a distribution function (or its moments). For example, a simulation model might yield a histogram of detection probabilities determined from a large number of target tracks, source levels, and environmental conditions. The obvious questions for this study are:

- Under given ensembling conditions, how sensitive are the performance predictions to the environmental acoustic (EVA) parameters?

Or, in other words,

- What is the level of accuracy (detail) needed in the estimate of EVA data as a function of the type (extent) of ensembling?

This question is addressed below. The results are not surprising to anyone who has thought about the problem, but have implications which should be (and are often not) taken into account in every performance/engagement analysis.

The simplest, most elementary, problem is treated first in great detail. The conclusions are then extended to more general cases.

3.1 Special Case

Assume the simplest type of detector, operating on a quantity to be called SN, which is some processed function of the signal and noise. This quantity SN is described deterministically as a function of range (R) from source to receiver, and detection occurs (for certain) when SN(R)>0. The source/receiver geometry as a function of time is the ensembling characteristic, and it is embodied in the range variable R(t). Because of the simple detector, the only property of SN(R) which matters is whether or not it exceeds zero. It can thus be reduced to a function which has values either 0 or 1. Suppose that SN(R) has only finitely many changes in value over the ranges 0 to $\hat{R}$, and that these changes occur at ranges:

$$R_0 = 0,\ R_1,\ R_2,\ldots,\ R_{N-1},\ R_N = \hat{R}.$$

The function SN can then be defined as:

$$SN(R) = \begin{cases} 0 & \text{for } R \in [R_{i-1},\ R_i),\ i \text{ odd} \\ 1 & \text{for } R \in [R_{i-1},\ R_i),\ i \text{ even} \end{cases}$$

Finally, let L_i denote the length of the intervals $[R_{i-1}, R_i)$:

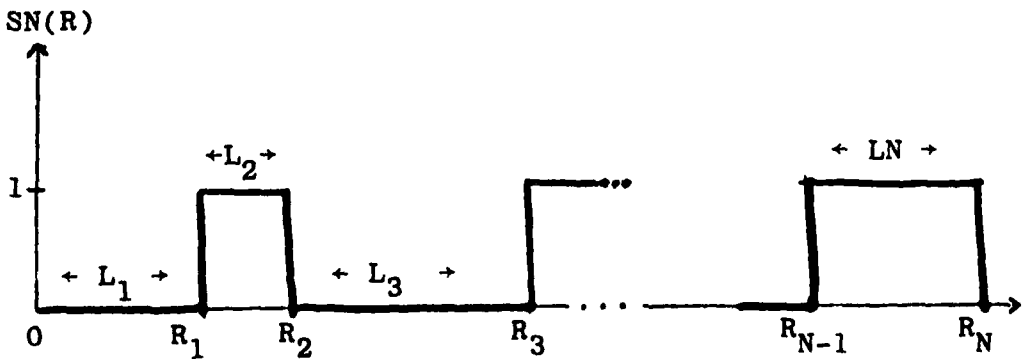

Note then that instantaneous and cumulative detection probabilities are calculated according to:

$$P_D(t) = 1 \text{ if } R(t) \in L_i \text{ for } i \text{ even}$$

$$CP_D(t) = 1 \text{ if } R(s) \in L_i \text{ for } i \text{ even, for some } s \in [0,t] .$$

If $R(t)$ is a random process, then so are $P_D(t)$ and $CP_D(t)$, and we consider their distributions for each t as functions of the distribution of $R(t)$.

Finally, a subtle point must be made. $P_D(t)$ for a deterministic $R(t)$ is simply

$$P_D(t) = P(SN(R(t)) > 0)$$

$$= \begin{cases} 0 & \text{if } R(t) \in L_i, \ i \text{ odd}, \\ 1 & \text{otherwise.} \end{cases}$$

If $R(t)$ is a random variable, then we define $P_D(t)$ as the <u>random variable</u>

$$P_D(t) = P(SN(R(t)) > 0) = \begin{cases} 0 \text{ when } R(t) \in L_i, \ i \text{ odd} \\ 1 \text{ otherwise.} \end{cases}$$

which takes on values of 0 and 1 only, with a distribution induced by that of $R(t)$ for each t. What some might call $P_D(t)$ (viz., $P(R(t) \in L_i, i \text{ even})$, is in our case the <u>expected value</u> of $P_D(t)$ over $R(t)$,

$$E(P_D(t)) = 1 \cdot P(R(t) \in L_i, i \text{ even}) + 0 \cdot P(R(t) \in L_i, i \text{ odd}).$$

The <u>distribution</u> of $P_D(t)$, over $R(t)$, is given by

$$\begin{cases} P(P_D(t) = 1) = P(R(t) \in L_i, i \text{ even}), \\ P(P_D(t) = 0) = 1 - P(P_D(t) = 1). \end{cases}$$

Similar considerations were made in Section 2.

3.1.1 Random Initial Range, Deterministic and Constant Speed

The relative source/receiver range is of form

$$R(t) = r_o + vt,$$

where v is constant and r_o is uniform on $[0, R_N]$. To eliminate boundary effects, we suppose that $V \geq 0$ and SN(R) is continued periodically to $R = \infty$.

Calculation of the basic MOE's is then straightforward.

$$P_D(t) = \begin{cases} 1 & \text{if}(r_o + vt) \epsilon L_i, \text{ i even} \\ 0 & \text{otherwise} \end{cases}$$

$$P\{P_D(t) = 1\} = P\{r_o + vt \epsilon L_i, \text{ i even}\} =$$

$$= \left(\sum_{i \text{ even}} L_i \Big/ \sum_{i=1}^{N} L_i\right) \equiv L_E/L$$

$$E\left\{P_D^k(t)\right\} = 1^k \cdot (L_E/L) + 0^k (L_0/L)$$

$$= L_E/L$$

$$\text{Var}\,(P_D(t)) = L_E/L - (L_E/L)^2 = (L_E/L) \cdot (L_0/L)$$

$$CP_D(t) = \begin{cases} 1 \text{ if } r_o \epsilon L_i, \text{ i even} \\ 1 \text{ if } r_o \epsilon L_i, \text{ i odd, and } (r_o + tv) > R_i \\ 0 \text{ if } r_o \epsilon L_i, \text{ i odd, and } (r_o + tv) \leq R_i \end{cases}$$

$$P\{CP_D(t) = 0\} = P(r_o \epsilon L_i,\ i \text{ odd; and } (r_o + tv) \le R_i)$$

$$= \sum_{i \text{ odd}} P\ (R_{i-1} \le r_o < R_i - tv)$$

$$= \sum_{i \text{ odd}} \max\left\{0, \left(\frac{L_i - tv}{L}\right)\right\} \qquad (3\text{-}1)$$

$$= \sum_{\substack{i \text{ odd} \\ L_i \ge tv}} \left(\frac{L_i - tv}{L}\right) .$$

Let $\{\hat{L}_i\}$ be a reordering of the odd-indexed L_i's such that for odd j,

$$\hat{L}_j \le \hat{L}_{j+2}.$$

Then $P\{CP_D(t) = 0\}$ is a piecewise linear function of t with nodes

$$\left(t = \hat{L}_j/v,\ j \text{ odd};\ P(CP_D(t) = 0) = \sum_{\substack{i \text{ odd} \\ i \ge j}} \frac{\hat{L}_i - tv}{L}\right)$$

and slopes of -kv/L, where k is the number of indices with $\hat{L}_i \ge tv$, as shown in Figure 3-1.

Of course, $P\{CP_D(t) = 1\} = 1\text{-}P\{CP_D(t) = 0\}$, which is again piecewise linear with the obvious nodes. Notice that

$$P\{CP_D(0) = 1\} = L_E/L = P\{P_D(t) = 1\},$$

$$P\{CP_D(t) = 1\} = 1 \text{ if } t > (L_i/v) \text{ for all odd } i.$$

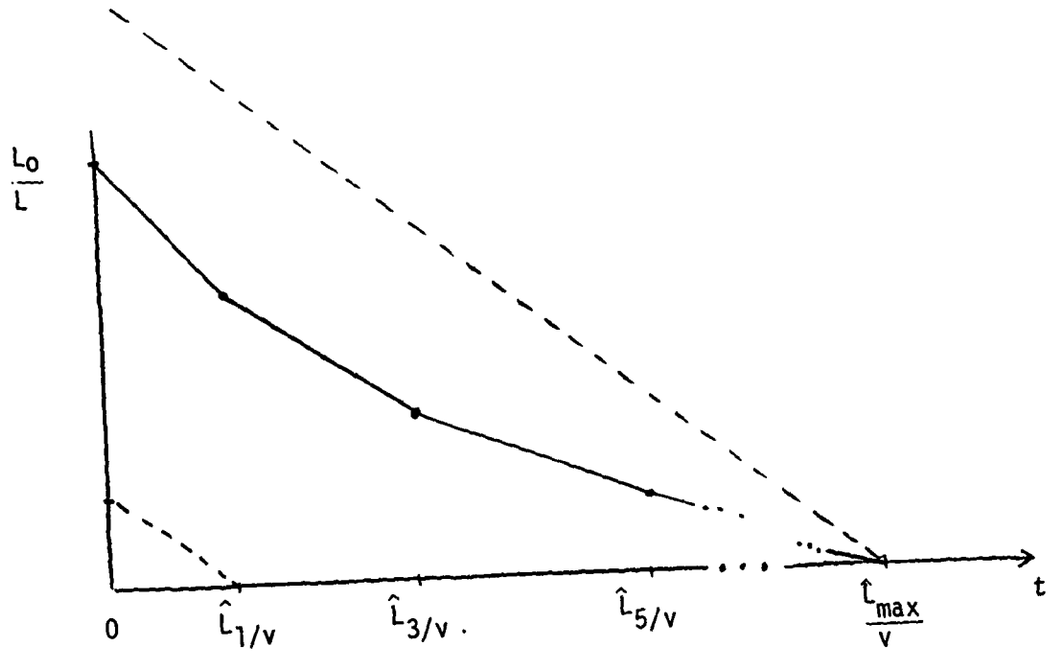

$P\{CP_D(t) = 0\}$

Figure 3-1

If $L_1 = L_3 = \ldots = L_{2j+1}$ for all j, then

$$P\{CP_D(t) = 0\} = \begin{cases} \left[\frac{N+1}{2}\right]\left(\frac{L_1 - tv}{L}\right) & \text{when } tv \le L_1 \\ 0 & \text{otherwise.} \end{cases}$$

Also, in any case,

$$\max\left\{0, \frac{\left[\frac{N+1}{2}\right]\left(\hat{L}_1 - vt\right)}{L}\right\} \le P\{CP_D(t) = 0\} \le \max\left\{0, \frac{\left[\frac{N+1}{2}\right]\left(\hat{L}_{MAX} - vt\right)}{L}\right\}$$

as shown in Figure 3-1 as dashed lines.

The moments of $CP_D(t)$ follow easily:

$$E\{(CP_D(t))^k\} = 1^k \cdot P(CP_D(t) = 1) + 0^k \cdot P(CP_D(t) = 0)$$

$$= 1 - P(CP_D(t) = 0).$$

3.1.2 Random Speed, Deterministic Initial Range

As above, let

$$R(t) = r_o + vt.$$

However, now fix r_o and let v be uniformly distributed on the interval $\left[v_1, v_2\right]$, where $0 < v_1 < v_2$. It is clear that $P_D(t)$, $P\{P_D(t)=1\}$, and hence $E\{P_D{}^k(t)\}$ are the same as before.

Likewise,

$$CP_D(t) = \begin{cases} 1, \text{ if } r_o \in L_i, \text{ i even} \\ 1, \text{ if } r_o \in L_i, \text{ i odd, and } r_o+tv > R_i \\ 0, \text{ if } r_o \in L_i, \text{ i odd, and } r_o+tv \leq R_i. \end{cases}$$

However,

$$P\{CP_D(t)=0\} = \begin{cases} 0, \text{ if } r_o \in L_i, \text{ i even} \\ 0, \text{ if } r_o \in L_i, \text{ i odd, and } r_o+tv_1 > R_i \\ \left(\frac{R_i-r_o}{t} - v_1\right) \Big/ (v_2-v_1), \text{ if } r_o \in L_i, \text{ i odd,} \\ \quad \text{and } r_o+tv_1 < R_i \leq r_o + tv_2 \\ 1, \text{ if } r_o \in L_i, \text{ i odd, and } r_o+tv_2 \leq R_i \end{cases} \qquad (3\text{-}2)$$

Thus $P\{CP_D(t)=0\}$ as a function of t is either the constant function zero (if $r_o \in L_i$, i even), or it consists of three segments - the constant function 1 for $t < \frac{R_i-r_o}{v_2}$, hyperbolic for $\frac{R_i-r_o}{v_2} < t < \frac{R_i-r_o}{v_1}$, and the constant function zero for $t > \frac{R_i-r_o}{v_i}$. This is shown in Figure 3-2.

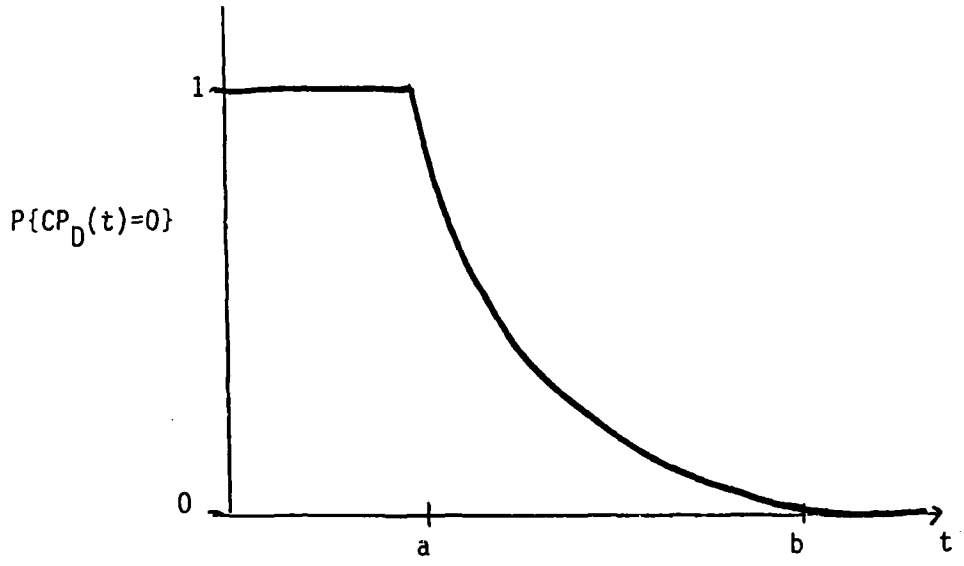

where $a = (R_i - r_o)/v_2$,

$b = (R_i - r_o)/v_1$

Figure 3-2

3.1.3 Random Speed, Random Initial Range

Suppose now that r_o and v are each uniformly distributed. Once again $P_D(t)$, $P\{P_D(t)=1\}$, $E\{P_D^k(t)\}$, and $CP_D(t)$ are the same as before. Recalling the result for a fixed speed, (3-1), we have

$$P\{CP_D(t) = 0\} = \int P\{CP_D(t)=0 \mid v\} \cdot P\{v\}\, dv$$

$$= \frac{1}{v_2-v_1} \int_{v_1}^{v_2} \sum_{\hat{L}_i \geq tv} \frac{\hat{L}_i - tv}{L}\, dv$$

$$= \frac{1}{v_2-v_1} \int_{v_1}^{v_2} \left(\sum_i \frac{\hat{L}_i - tv}{L} - \sum_{\hat{L}_i < tv} \frac{\hat{L}_i - tv}{L} \right) dv$$

$$= \sum_i \frac{\hat{L}_i - \frac{1}{2}t(v_1+v_2)}{L} - \frac{1}{v_2-v_1} \int_{v_1}^{v_2} \sum_{\hat{L}_i < tv} \frac{\hat{L}_i - tv}{L}\, dv \qquad (3\text{-}3)$$

To carry this further, consider three cases:

Case I: $0 \leq t \leq \frac{\hat{L}_i}{v_2}$ (i.e., $\hat{L}_i > tv$, for all i and for all $v \in [v_1, v_2]$)

Since there are no $\hat{L}_i < tv$, (3-3) becomes

$$P\{CP_D(t)=0\} = \sum_{\hat{L}_i > \frac{1}{2}t(v_1+v_2)} \frac{\hat{L}_i - \frac{1}{2}t(v_1+v_2)}{L}$$

$$= P\{CP_D(t)=0 \mid v=\tfrac{1}{2}(v_1+v_2)\} \qquad (3\text{-}4a)$$

This, as seen in section 3.1.1, is linear with slope $-kv/L$.

Case II: $t > \frac{L_m}{v_1}$ (i.e., $\hat{L}_i < tv$, for all i and for all $v \in [v_1, v_2]$

Since all $\hat{L}_i < tv$, (3-3) becomes

$$P\{CP_D(t)=0\} = 0. \qquad (3\text{-}4b)$$

Case III: $\frac{\hat{L}_1}{v_2} < t < \frac{\hat{L}_m}{v_1}$

For a given t, choose j such that $\hat{L}_j = \max_{\hat{L}_i > tv_2} \{\hat{L}_i\}$.

Then from (3-3)

$$P\{CP_D(t)=0\} = \sum_i \frac{\hat{L}_i - \frac{1}{2}t(v_1+v_2)}{L} - \frac{1}{v_2-v_1} \cdot \sum_{i=1}^{j} \int_{\max\{\hat{L}_i/t, v_1\}}^{v_2} \frac{\hat{L}_i - tv}{L}\, dv$$

$$= \sum_i \frac{\hat{L}_i - \frac{1}{2}t(v_1+v_2)}{L} - \sum_{i=1}^{j} \frac{v_2 - \max\{\frac{\hat{L}_i}{t}, v_1\}}{v_2 - v_1} \cdot \frac{\hat{L}_i - \frac{1}{2}t(v_2 + \max\{\frac{\hat{L}_i}{t}, v_1\})}{L}$$

Next, choose k such that $\hat{L}_k = \min_{\hat{L}_i > tv_1} \{\hat{L}_i\}$. Then

$$P\{CP_D(t)=0\} = \sum_{i=k}^{m} \frac{\hat{L}_i - \frac{1}{2}t(v_1+v_2)}{L}$$

$$- \sum_{i=k}^{j} \frac{v_2 - \hat{L}_i/t}{v_2 - v_1} \cdot \frac{\hat{L}_i - \frac{1}{2}t(v_2 + \hat{L}_i/t)}{L} \cdot \qquad (3\text{-}4c)$$

Finally, it can be shown that $P\{CP_D(t)=0\}$ and its first derivative are continuous for $t>0$. Higher order derivatives in general, however, are not continuous. Figure 3-3 shows a particular $P\{CP_D(t)=0\}$. The vertical dashed lines delineate the intervals over which all derivatives are continuous.

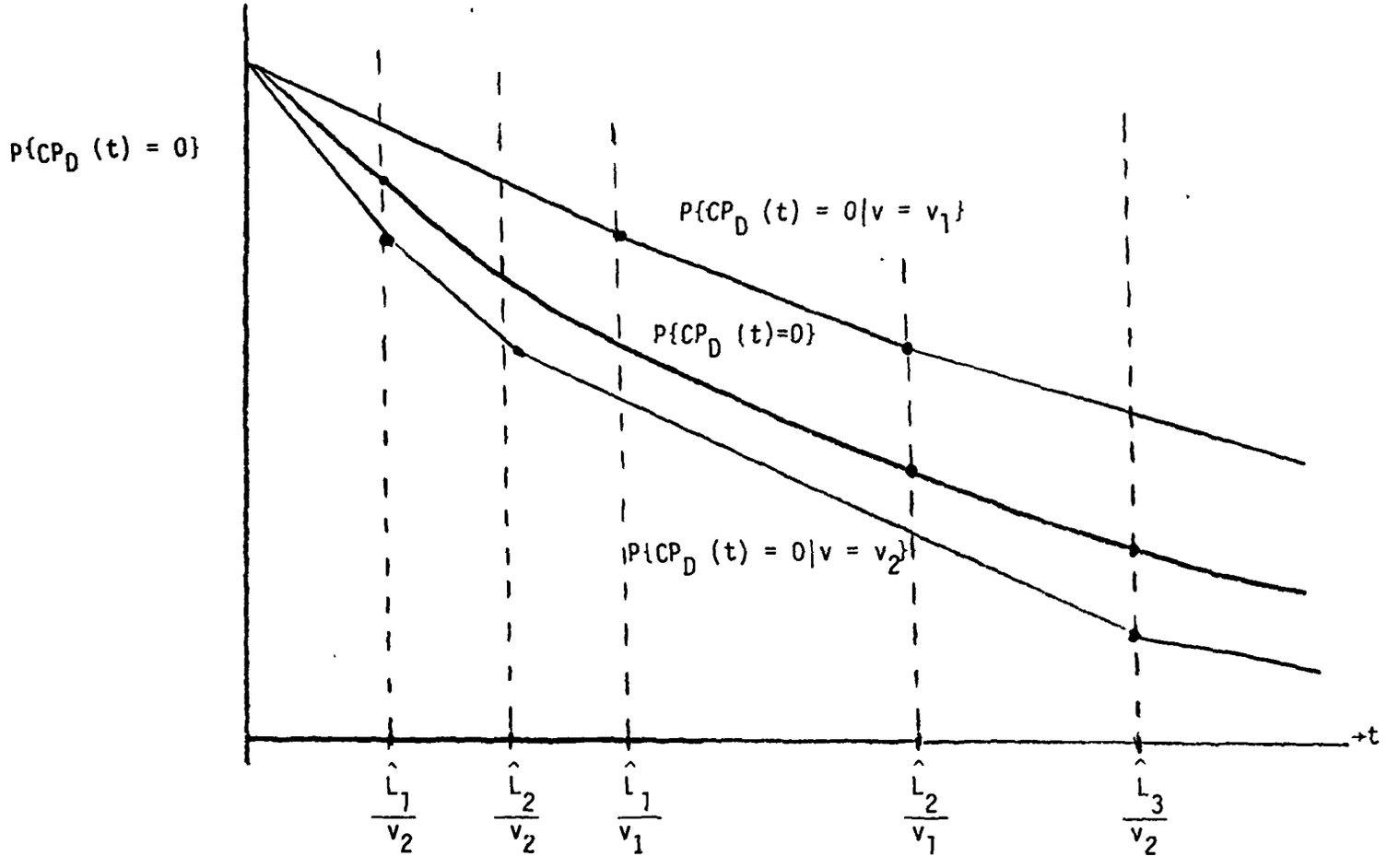
P{CP_D (t) = 0}
P{CP_D (t) = 0|v = v_1}
P{CP_D (t)=0}
P{CP_D (t) = 0|v = v_2}
t
L̂_1/v_2
L̂_2/v_2
L̂_1/v_1
L̂_2/v_1
L̂_3/v_2

Figure 3-3

3.2 Extrapolations

The special case given above was examined in detail for several reasons:

- o It is as simple a case as can be contrived, and yields closed-form solutions (equations (3-1), (3-2) and (3-4)).
- o The form of the solutions allows for direct examination of the sensitivity of the detection probabilities to the input scenario for important types of ensembling.
- o With some modifications, the results can be easily extended to more general, realistic problems.

Consider next some observations based on these results.

Note first that SN(t) is determined completely by the interval lengths $\{L_i\}$ and the range rate R(t). When R(t) is a random process, so is SN(t). If R(t) is Markov, then SN(t) is also Markov. Similarly, randomness in $\{L_i\}$ induces randomness in SN, for deterministic R(t).

Next consider the association of the forms of R(t) with properties of SN, usually identified as fluctuations:

Special Case	Extrapolation
Random initial range	Imprecise location of peaks and nulls in SN(R)
Random, but constant speed	Imprecise scaling of periods of SN
Random range rate (R(t))	Random periods and amplitudes for SN
Periodic speed	Periodic variations in SN

Formulas such as (3-1) or (3-4) can then be used to determine precision needed in the definition of the intervals $\{L_i\}$, i.e., the amount of detail in the description of SN(R). If the ensembling (randomness in R(t)) leads to insensitivity of detection probabilities to anything but the average lengths of the $\{L_i\}$, then a prediction of the EVA parameter, SN, need not be very accurate in representing anything but those average lengths.

SECTION 4
TRANSMISSION FLUCTUATION PROPERTIES

In a previous investigation (Ref 4-1) it was determined that the value of the random-process (or any other) approach to predicting system performance was critically dependent on the accuracy of "input" data:

- mean transmission loss (TL), at the beamformer output,
- mean beam noise (BN),
- the temporal statistics of TL and BN fluctuations (at a level of detail consistent with the amount of ensembling, as discussed above).

Current acoustic models can, in many cases, predict the mean values with adequate efficiency and accuracy, given a good description of the important environmental parameters (e.g., sound speed, bottom properties, noise sources). Furthermore, there are models which can estimate the temporal fluctuations in detail (again, see Ref 4-1). These models are based on the physical mechanisms, and (at least in the case of TL) have shown good agreement with measurements.

Unfortunately, fluctuation-prediction routines generally require substantial amounts of computer calculations. The reason is that the models act as "simulators," estimating the time series of signal or noise, which in turn are statistically analyzed to distill the important

parameters. In this section and the next, approaches for predicting certain key statistics of TL and BN with minimal computational effort are proposed.

In summary, consider two methods for estimating TL and BN properties for performance analyses:

(a) Use computer models to "simulate" the detailed time series of TL or BN. The results can be used directly in sonar simulations, or else important properties can be obtained from time-series analysis to be used as inputs to random-process models (which in turn are often used in a Monte Carlo sense to provide replicas of the original time series).

(b) Apply existing, efficient models to estimate mean values of TL and BN. Use consistently efficient calculations (proposed below) to predict important fluctuation statistics for use in random process (or other) performance predictions.

For any practical application, (b) should be an obvious choice over (a). This section and Section 5 describe algorithms for estimating TL and BN fluctuation properties.

4.1 Transmission Fluctuations: Assumptions and Basic Models

The emphasis here is on passive sonars, employing narrowband processing at acoustic frequencies from about 50

to 2000 Hz or more (for long range detection, the lower end of the frequency scale is most useful). Typically the signal processor coherently integrates (filters) for several or more seconds and then incoherently averages the resultant samples for several minutes. Interest then is in characterizing the properties of the average envelope of signal (and noise). [Ref 4-1 discusses processing and detection algorithms for this problem].

A stable CW source signal is assumed in this study. Fluctuations in the received signal are thus attributed to transmission phenomena, and a number of mechanisms are possible. Consider two classes: those related to the motion or dynamics of the ocean medium and those related to motion of the source and receiver. There seems to be some concensus in the community that when there is significant relative range rate between source and receiver, the latter class dominates, and the mechanism is the variation in the received multipath interference field (see, e.g., References 4-2 through 4-4). The model considered here is based on this assumption.

Following Reference 4-1, the usual plane-wave ray formulation for signal multipaths with fixed receiver and CW source is:

$$s(t) = \sum_n A_n \exp[i(\omega t - k_n r + \phi_n)] \qquad (4\text{-}1)$$

where A_n is RMS pressure, $k_n = k\cos\theta_n$, k is wavenumber, r is range, ω is angular frequency, θ_n is ray angle at the

receiver, and ϕ_n is a phase angle determined by travel time and phase shifts along the path. Intensity is then proportional to

$$\frac{1}{T}\int_0^T s(t)s^*(t)dt. \qquad (4\text{-}2)$$

Current ray (and wave) models have been shown able (at least at lower frequencies) to predict quite accurately the components of (4-1), with uncertainty principally in the relative phases (ϕ_n) of paths with significantly different histories (see, e.g., References 4-5 and 4-6).

When the source location is fixed, a moving receiver simply samples the static field of (4-1) in range. For A_n and k_n locally range independent and r(t) the time-dependent distances,

$$s(t) = \sum_n A_n \exp[i(\omega t - k_n r(t) + \phi_n)]. \qquad (4\text{-}3)$$

The distributions of pressure and intensity over time are thus determined directly from (4-3) and (4-2). Special cases discussed in Ref 4-1 yield chi-square (or gamma) and non-central chi-square distributions with 2 degrees of freedom for the intensity fluctuations.

Continuing with the fixed source case, notice that (4-3) and (4-2) give a time series for intensity:

$$I(t) = \sum_n A_n^2 + \sum\sum_{m \neq n} A_m A_n \cos\,[(k_m - k_n)r(t) + \hat{\phi}_{mn}]. \qquad (4\text{-}4)$$

where

$$k_m - k_n = k(\cos\theta_m - \cos\theta_n).$$

The intensity fluctuations are thus driven by terms of form

$$A_m A_n \cos[(k_m - k_n) r(t)].$$

Following Reference 4-7, define a "spatial spectrum" for I as

$$I(k_m - k_n) = A_m A_n,$$

which identifies the dominant oscillations of I in range or in time (based on r(t)). Just how the component sinusoids combine depends on the relative phases ($\hat{\phi}_{mn}$) and the amplitudes $A_m A_n$.

The effect of receiver motion on s(t) can be viewed in two ways, the most obvious being that the phase of each path (n) becomes modulated by $k_n r(t)$, in general a slowly varying function of t. If, on the other hand, r(t) is linear in t, say r(t) = vt, then the n-th component of s(t) has constant phase and frequency given by:

$$\omega_k \equiv (\omega - k_n V) = (1 - \frac{V\cos\theta_n}{c}). \qquad (4\text{-}5)$$

This is the classical Doppler-shifted frequency. Formula (4-3) thus shows components of pressure with individually Doppler-shifted frequencies; interference among the components is determined for intensity from (4-4).

While the case of receiver motion is straightforward, the source-motion problem is not. In fact, a very large amount of effort has been expended in the investigation of the difference bewteen the two problems and of methods for modeling transmission loss fluctuations induced by the moving source (see, e.g. References 4-8 through 4-12). Spofford has, under this contract effort, endeavored to determine the important features of source-motion effects and documented the results in a separate report (Ref 4-13). His findings are summarized next:

> In the context of (4-1), the received pressure for a fixed source and moving receiver has form
>
> $$s(t) = \sum_k A_k \exp[i(\omega_k t - \omega T_k)],$$
>
> while that for a fixed receiver and moving source is:
>
> $$s(t) = \sum_k A_k \exp\ [i\tilde{\omega}_k (t - T_k)],$$
>
> where
>
> $$\tilde{\omega}_k = \frac{\omega}{1 + v' \dfrac{\cos\theta'_R}{c}}$$
>
> Here T_k is a reference travel time, v' is radial source speed, and θ'_k is ray angle at the source.
>
> The moving-source condition can thus be modeled in a range-independent environment in the same way as the moving-receiver case, i.e., by sampling the static field originating at the receiver (in a reciprocal sense) at the source's relative speed (v'). The errors thus incurred are:
>
> - The Doppler-shifted frequencies ω_k and $\tilde{\omega}_k$ are slightly different (second order in v/c).
>
> - The relative phase between two paths is distorted, with difference
>
> $k \cdot v \cdot (T_k \cos\theta_k - T_j \cos\theta_j)$.

The precise locations of peaks and nulls are thus perturbed.

The first error is known, and of little consequence. The second is unimportant for most applications.

In summary, the statistics of fluctuations in transmission loss caused by source/receiver motion can be derived by generating the static field from a fixed source and then sampling the field locally in range at the relative source/receiver range rate. The first-order statistics and spectra of the envelope fluctuations can be found from the range-sampled data with error of smaller order than v/c.

4.2 Method for Estimating Fluctuation Statistics

Under the assumptions of the preceding subsection, a method for efficiently calculating statistics of transmission-loss fluctuations is presented below. Focus is on the variance and range periodicities (spectrum) of the received intensity, employing an approach developed by Spofford (Ref 4-14). The method accounts for certain effects of processor averaging and beamforming. A subsequent section compares results of the method with statistics generated by detailed TL models and discusses the sensitivity of the output statistics to environmental inputs.

Consider two types of multipath interference:

(a) Interference within an Order. An arrival order is a group of paths which differ in history by a boundary reflection near the

source and/or the receiver. In the interesting case that the source or receiver is near the boundary, two or more paths have nearly identical travel times, and persistent periodicities in range are observed. Surface-image interference (SII) is an example of this effect.

(b) Inter-Order Interference. In this case, paths of different orders connect source to receiver, and generate an interference field. This is the usual case for bottom-bounce propagation.

For the first case (a), the coherent sum of paths often results in "slow" range variations which are treated as deterministic and included in the prediction of mean TL. Under the assumption of constant sound speed between a source at depth z_1, a receiver at depth z_2 and a pressure-release surface, the SII effect yields an intensity of form

$$I = 4I_o \sin^2(kz_1 \sin\theta_1) \sin^2(kz_2 \sin\theta_1) \qquad (4\text{-}6)$$

where I_o is the intensity for an individual path and θ_1 is angle at source or receiver (more general results are found in Ref 4-15). The change of θ_1 with range yields periodic fluctuations for I; the fluctuation period is large when kz_i is small. When the inter-order case is treated below, such fluctuation scales must be examined to determine if the slow variations are to be viewed as part of the mean TL or not. The FACT model (Ref 4-16) includes SII, but not inter-order interference.

Turn now to the more general type of interference (b), and recall equation (4-4), rewritten in terms of I_m, the squared RMS pressure or intensity for the m-th path:

$$I = \sum_m I_m + \sum_{m \neq n} \sum (I_m I_n)^{1/2} \cos[(k_m - k_n)r + \phi_{mn}] \qquad (4\text{-}7)$$

The range-averaged intensity is given by

$$\langle I \rangle = \sum_m I_m,$$

and the "relative" intensity by

$$\delta I = \frac{I}{\langle I \rangle}, \qquad (4\text{-}8)$$

a measure of the fluctuations of I. Notice that δI has a mean value of one and variance (in range) of

$$\sigma^2 = 1 - \left(\frac{\sum I_n^2}{(\sum I_n)^2} \right) . \qquad (4\text{-}9)$$

These expected values presume an average in range sufficient to sample full cycles of the cosine terms in (4-7). When this is not the case for certain paths (e.g., when slow variations of type (a) occur), then their contribution to the variance must be excluded from (4-9). On the other hand, when the signal processor's integration time is greater than a cycle of interference (as determined from range rate), then corresponding contributions should be omitted in (4-9). Such modifications are discussed further below in the context of range periods.

Refer again to equation (4-4) (or (4-7)). As noted earlier, the intensity is seen as the (phased) sum of sinusoids with range periods ρ determined from

$$(k_m - k_n)\ \rho_{mn} = 2\pi$$

or

$$\rho_{mn} = \frac{\lambda}{\cos\theta_m - \cos\theta_n} \cdot \qquad (4\text{-}10)$$

The relative "power" associated with this period is $I_m I_n / \langle I \rangle^2$, and the sum of all powers

$$\left(\sum_{m \neq n} \sum I_m I_n\right) / \langle I \rangle^2 \qquad (4\text{-}11)$$

is the variance (σ^2) of δI. In other words, the Fourier power spectrum for (4-7) in the variable r consists of discrete components with periods ρ_{mn} and power $I_m I_n$. As usual, the variance of the process is equal to the sum of the component powers (Parseval's Theorem). If certain components are to be omitted (because their oscillations are too slow or too fast, or their angles are outside the aperture of source or receiver), they are removed from the spectrum (i.e., added to the "d.c." component) and thus do not contribute to the variance.

A computer routine has been developed to perform the calculations described above, including SII effects and accounting for elimination of fluctuation periods outside a selected interval. A typical case costs about $0.50 for computer execution. The mechanics of the program are summarized next.

Intervals of allowable range period and angles at source and receiver are inputs. A ray trace is performed for the local sound speed, so that ray cycle distance (X), arrival angle (θ_2), and bottom-intersection angle (θ_B) can be found as functions of source angle (θ_1). For a given range (R), the intensity ($I_m(\theta_1)$) of each arrival is estimated. Range periods from (4-10) and associated "powers" can then be calculated. When a specific combination of paths has period greater than that allowed by the preselected interval, modifications are made to ensure that the power and variance are correct; an example follows.

Suppose paths 1 and 2 have ρ_{12} larger than allowed. The component $I_1 I_2$ is then removed from the spectrum and an estimate of the coherent sum of the paths made. In most cases such paths are of the same order, and SII is important, so that (4-6) can be applied to replace the two (or more) paths by a single new path with intensity $\hat{I}_1$. Combinations of paths 1 and 2 with those of other orders (say, path 3), must likewise be combined. In the computer code, paths are grouped by order and the correction of (4-6) made at the start when appropriate.

Once the spectrum is corrected, the range periods and relative importance are directly available. At this point, the effects of the signal processor can be incorporated--by eliminating components with range periods smaller than allowed. Finally, the variance is found from (4-11).

In summary, an efficient computer code has been developed to extract the important statistical properties of transmission-loss fluctuations caused by source/receiver

motion in multipath conditions. Examples, comparison with detailed TL calculations, and a sensitivity analysis follow in the next subsections.

4.3 Comparison with TL Model Results

Predictions by the routine described above were compared with the output of a detailed, fully coherent ray-trace model. The test case and results are summarized in this subsection.

The TL model employed is a special version of FACT (Ref 4-16) called "CFACT", in which all paths are summed coherently. Note at the outset that the cost of the single computer run exceeded $200, as compared to the usual FACT (semi-coherent) cost of about $1. and that of the fluctuation routine of less than $1. The details of the environmental and model data follow:

- The sound-speed profile is based on a North Atlantic measurement, and is characterized by a thin mixed layer above a weak thermocline, and pressure gradient from about 800 m to the ocean floor at 3600 m.

- The bottom is flat, with loss at 60 Hz corresponding to FNWC Class 1: no loss to 19° grazing angle, 6 dB per bounce beyond 52°, and a linear combination between.

- TL was calculated every 0.04 nm to a maximum range of 130 nm for a source at 150 feet, receiver at 500 feet, and frequency of 60 Hz.

- To determine fluctuation statistics, a 2 nm intensity average of TL was computed (TL), and removed from TL. The resulting function of range corresponds to the normalized intensity

$$\delta I(R) = I(R)/\langle I \rangle .$$

- δI was sampled in range over preselected range intervals, and the resulting sample sets used to compute the variance and range periods (spectrum).

The routine developed for this study was also used to generate σ^2 and ρ for the same inputs. Results of the comparison follow.

First, note that since the bottom is perfectly reflecting for grazing angles from 0^o to 19^o, there are at least two dominant bottom-bounce orders of nearly equal intensity at most ranges.

Figure 4-1 plots the dominant range periods versus range, as precicted by the fluctuation routine, while Table 4-1 compares these predictions with CFACT results; agreement is good. Consider next that as the range increases, the number of arrival orders does also. The result is interfering arrivals whose periods while possibly not dominant are still of some importance. To determine how well the fluctuation routine predicts these less powerful fluctuation periods, the range interval 100-130 nm is examined in

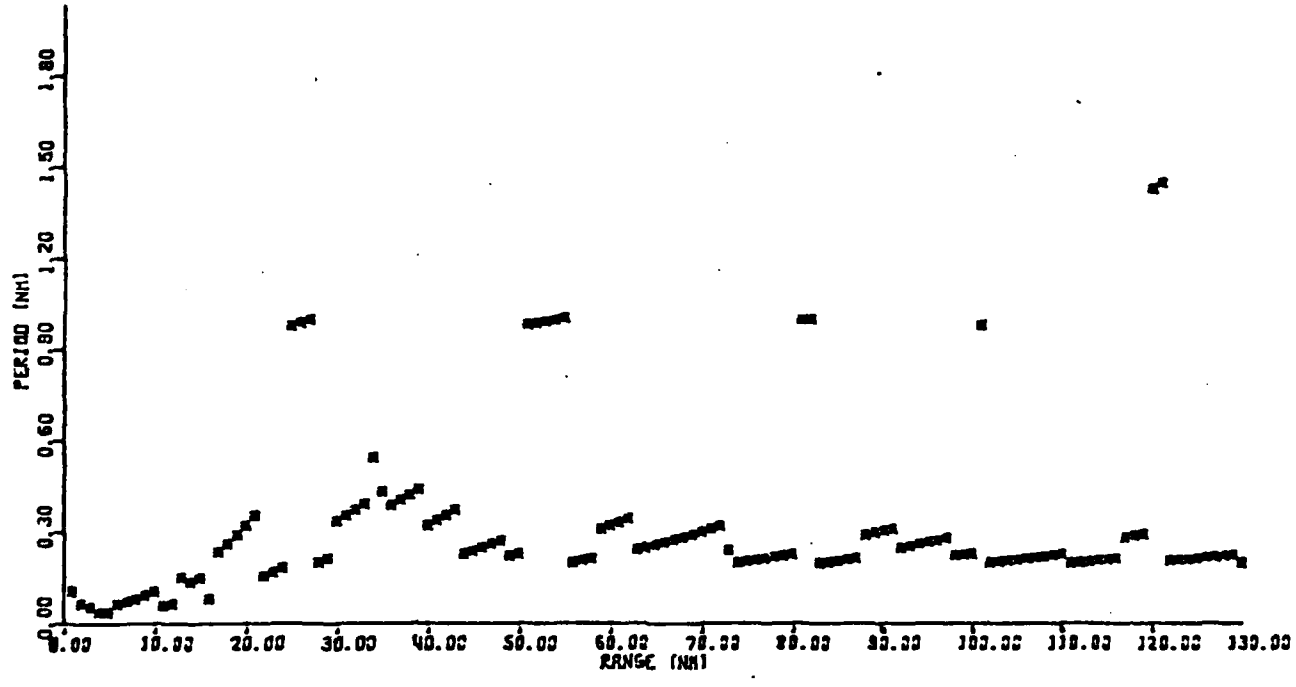

Figure 4-1
Fluctuation-Routine Prediction of Dominant Range Periods

Table 4-1

COMPARISON OF PREDICTIONS OF DOMINANT RANGE PERIODS

Range Interval (nm)	Dominant ρ for CFACT Data (nm)	Dominant ρ-Interval From Fluctuation Routines (nm)
12 - 20	0.25 - 0.29	0.23 - 0.31 at 45% of the ranges
25 - 43	0.25 - 0.36	0.30 - 0.44 at 68% of the ranges
45 - 70	0.27 - 0.34	0.21 - 0.34 at 73% of the ranges
100 - 130	0.28 - 0.32	0.19 - 0.23 at 80% of the ranges

greater detail. Figure 4-2 shows the dominating ρ's as computed by the routine at each range step. The ■'s represent the primary periods at each range while the x's are secondary periods (those with power within 5 dB). As noted previously, the primary range period for the CFACT data is 0.29, about which most of modeled results are centered. However, the spectrum also shows fluctuation periods whose power is within 4-5 dB of the dominant period at about 1.2 nm and 0.75 nm. Such results are reflected in the figure.

Turn next to the predictions of total variance. Figure 4-3 compares σ^2 for the fluctuation routine (.'·.) and the CFACT model (⊢—⊣). The length of the bar indicates ensembling interval. Agreement is poor beyond 20 nm for the following reason. The isospeed approximation for SII (equation 4-6) used in the fluctuation routine yields 3-4 arrival orders of about the same intensity, and hence a variance of about 0.7, at many ranges beyond 20 nm. An exact solution, based on the true sound-speed profile and reflected in the CFACT results, shows only 2 orders (and thus a variance of 0.5). While the fluctuation periods are nearly unchanged, their powers and sum (variance) are significantly different. A routine incorporating a better approximation for SII yields the x's in Figure 4-3, with good agreement.

In summary, for a test case with CFACT emphasizing interference of bottom-bounce orders, the fluctuation-routine predictions of ρ and σ^2 are quite satisfactory, and generated at a small fraction of the cost of running CFACT.

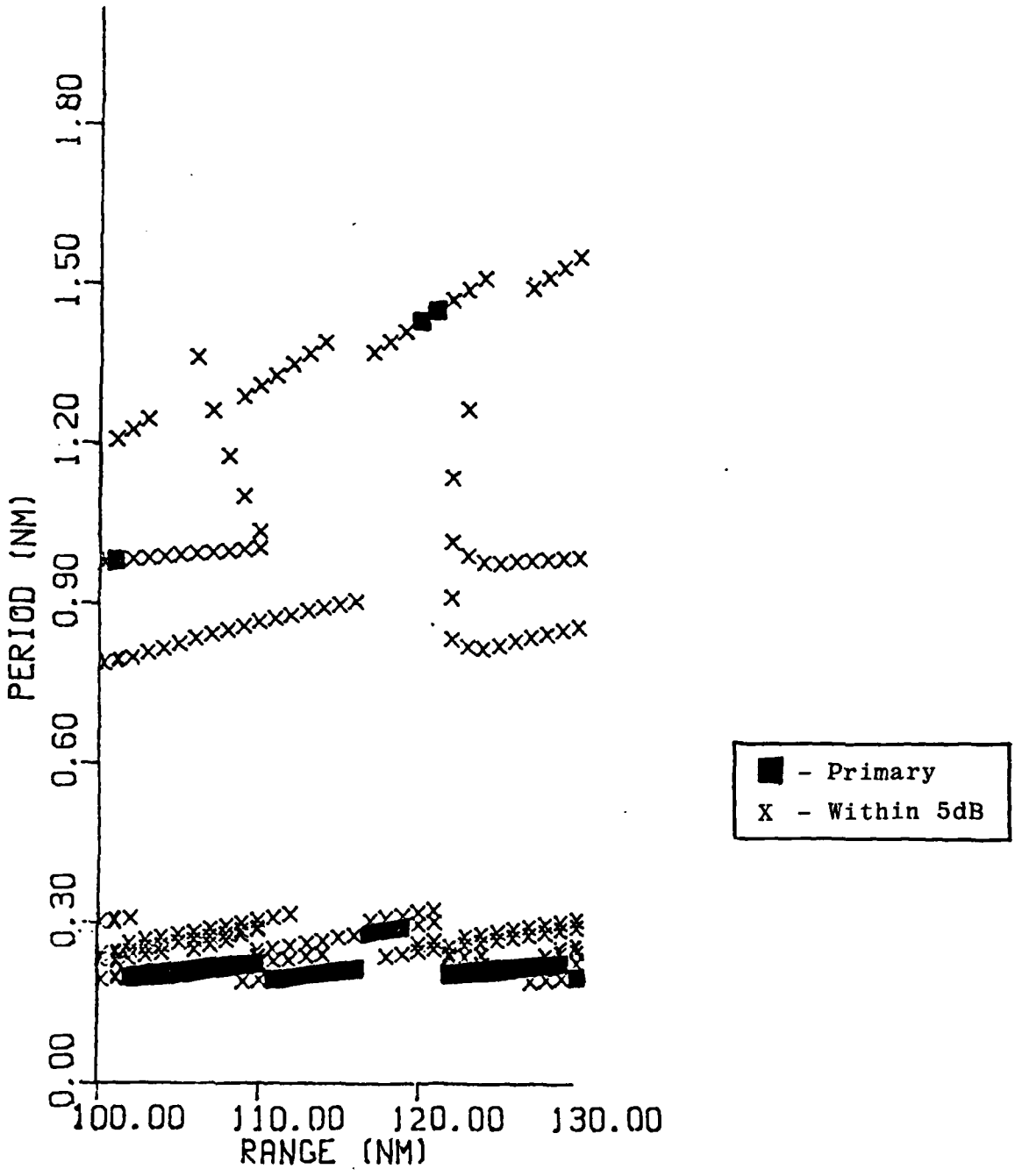

Figure 4-2
Fluctuation Routine Predictions of Range Periods

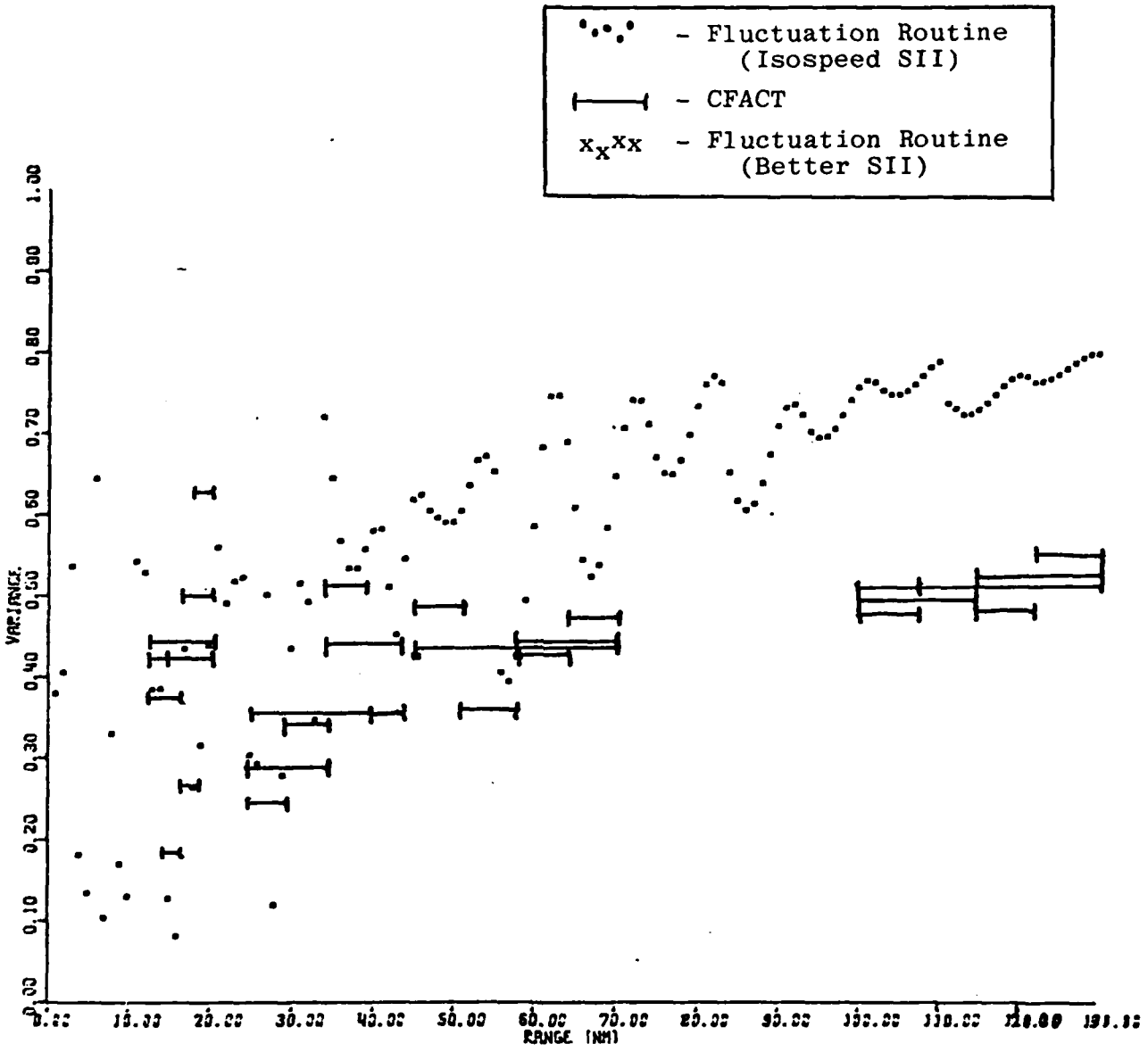

Figure 4-3
Comparison of Predicted Fluctuation Variances

4.4 Sensitivity Analysis

The previous subsections have endeavored to show that the fluctuation model has a sound basis in physics and produces reasonably accurate results in comparison with detailed TL model predictions for typical shallow-source/receiver, low-frequency scenarios. Of interest now is the sensitivity of model output to the various input parameters.

There are five basic inputs to the fluctuation model:

(1) Frequency
(2) Source depth
(3) Receiver depth
(4) Sound speed profile
(5) Bottom loss function

Although each of these individually affects the calculations, it is often the case that changes in several inputs act in concert to alter the output. To illustrate the sensivities of the model and to help develop a general characterization of the fluctuations, a special case is studied in detail next.

4.4.1 Special Case

Consider the scenario:

(1) Frequency = 25 Hz
(2) Source depth = 500 ft
(3) Receiver depth = 60 ft

(4) Sound speed profile is based on a North Pacific measurement. It features a thin mixed layer, a classic thermocline to the axis at about 1000 m and pressure gradient to the bottom at 6000 m.

(5) Bottom loss is 6 dB per bounce independent of grazing angle.

Concentate on multi-order bottom bounce propagation. For these inputs the model produces predictions for fluctuation period and variance as shown in Figure 4-4 and 4-5 respectively. Surface-image interference is an important contributor to these results, and Figure 4-6 shows the isospeed approximation (Equation 4-6) for $I(\theta)$ under the given frequency, source, receiver conditions, but without bottom loss. The angle at the receiver which grazes the bottom is approximately 10.7^{o} and has a ray-path of 35 *nm*. Shallower angles correspond to waterborne paths, which are of little interest here because of their long periods. On the other hand, angles that are too steep will suffer many bottom bounces even at short range, and be too lossy to matter here. The conclusion is that the dominant range period (within a scaling factor of frequency) results from interaction of arrivals with angles which are small (above 10.70) and which correspond to peaks in Figure 4-6.

At the shorter ranges (to 40 or 50 nm) where the separation between arrival angles is greatest, it is likely that their exists an arrival angle near 30^{o} that has not been attenuated too greatly by bottom interaction. Also, because of the large arrival angle separation it is unlikely that there are two arrivals near the 17.5^{o} peak. Hence

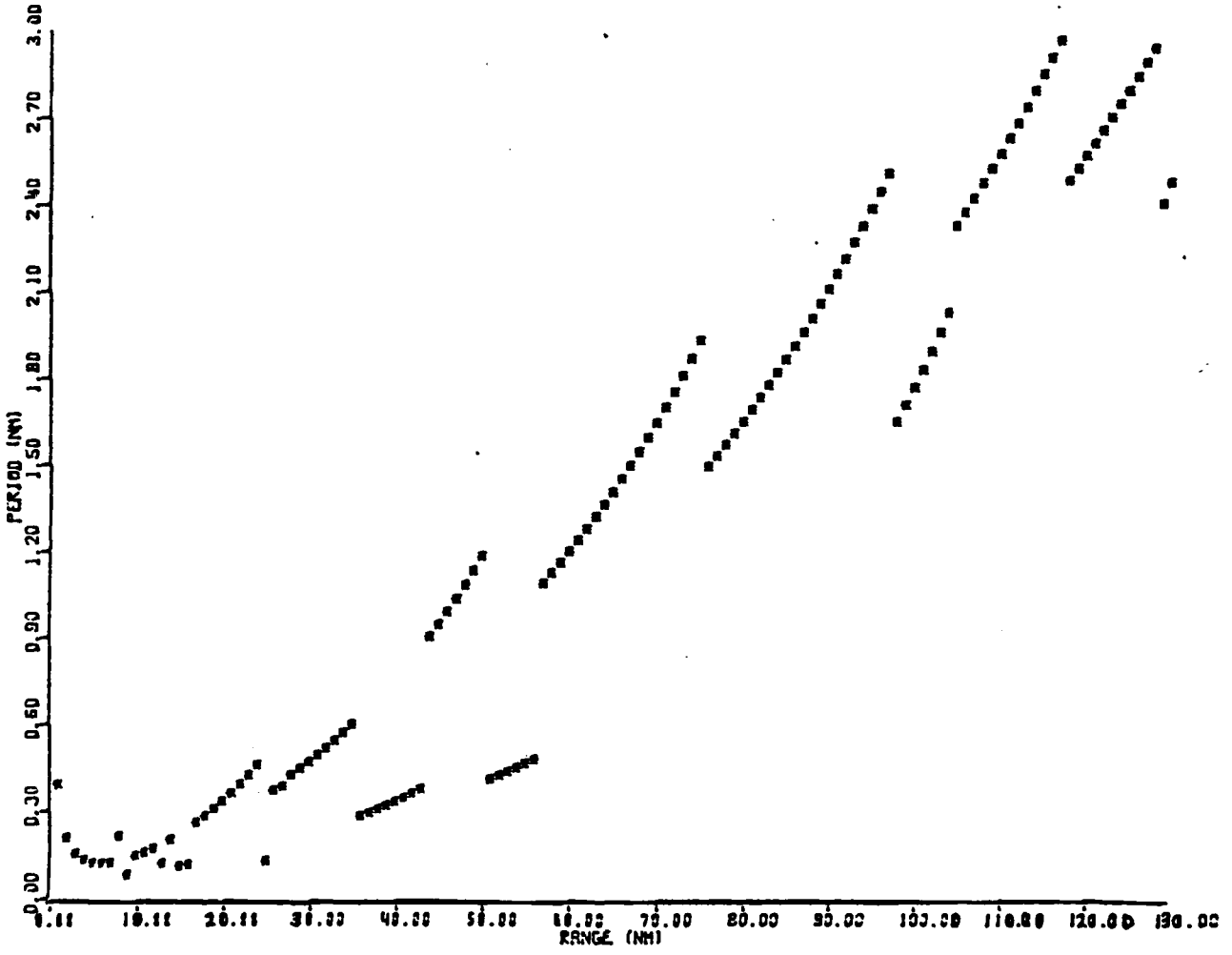

Figure 4-4
Dominant Range Periods for Special Case (25 Hz)

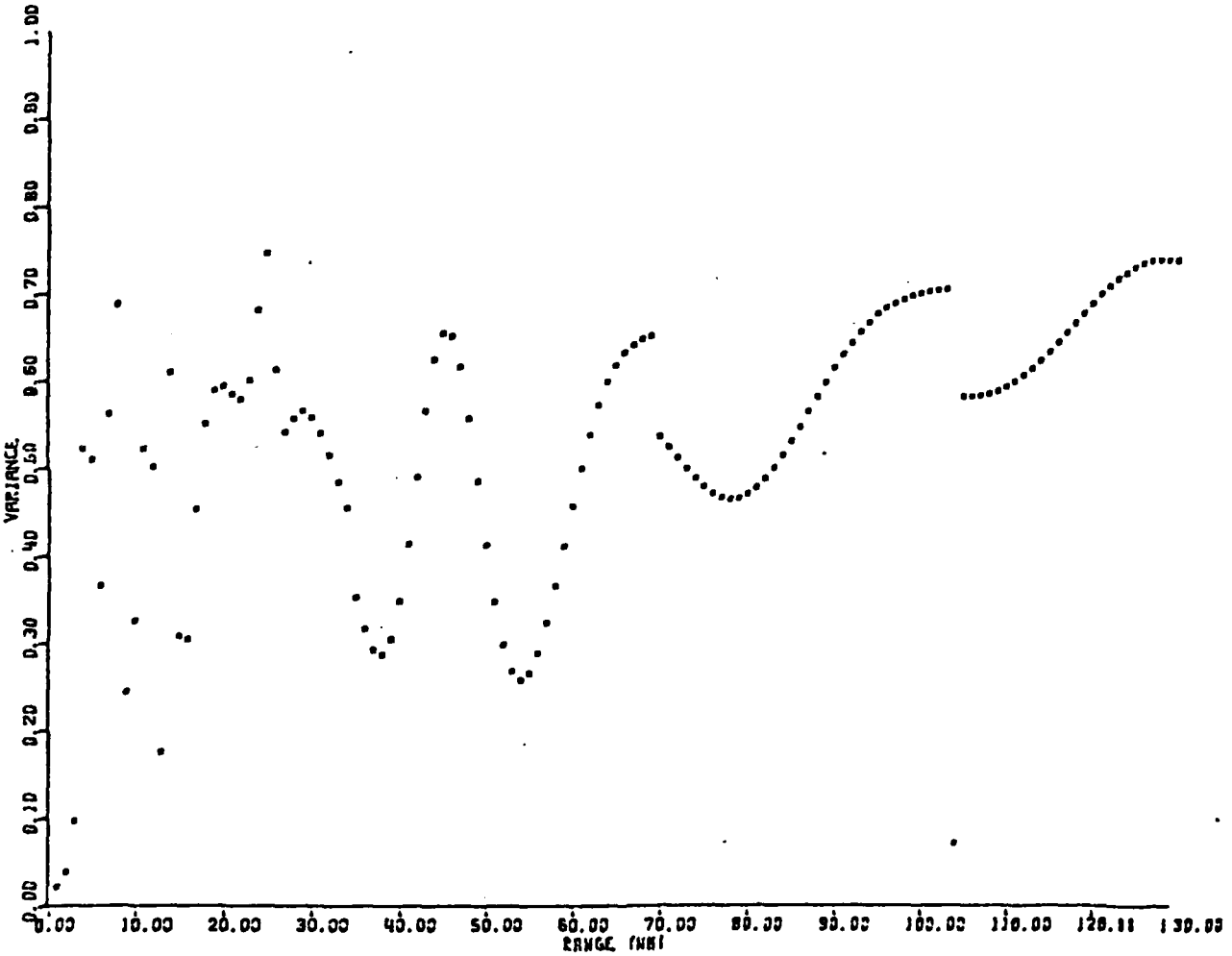

Figure 4-5
Variances for Special Case (25 Hz)

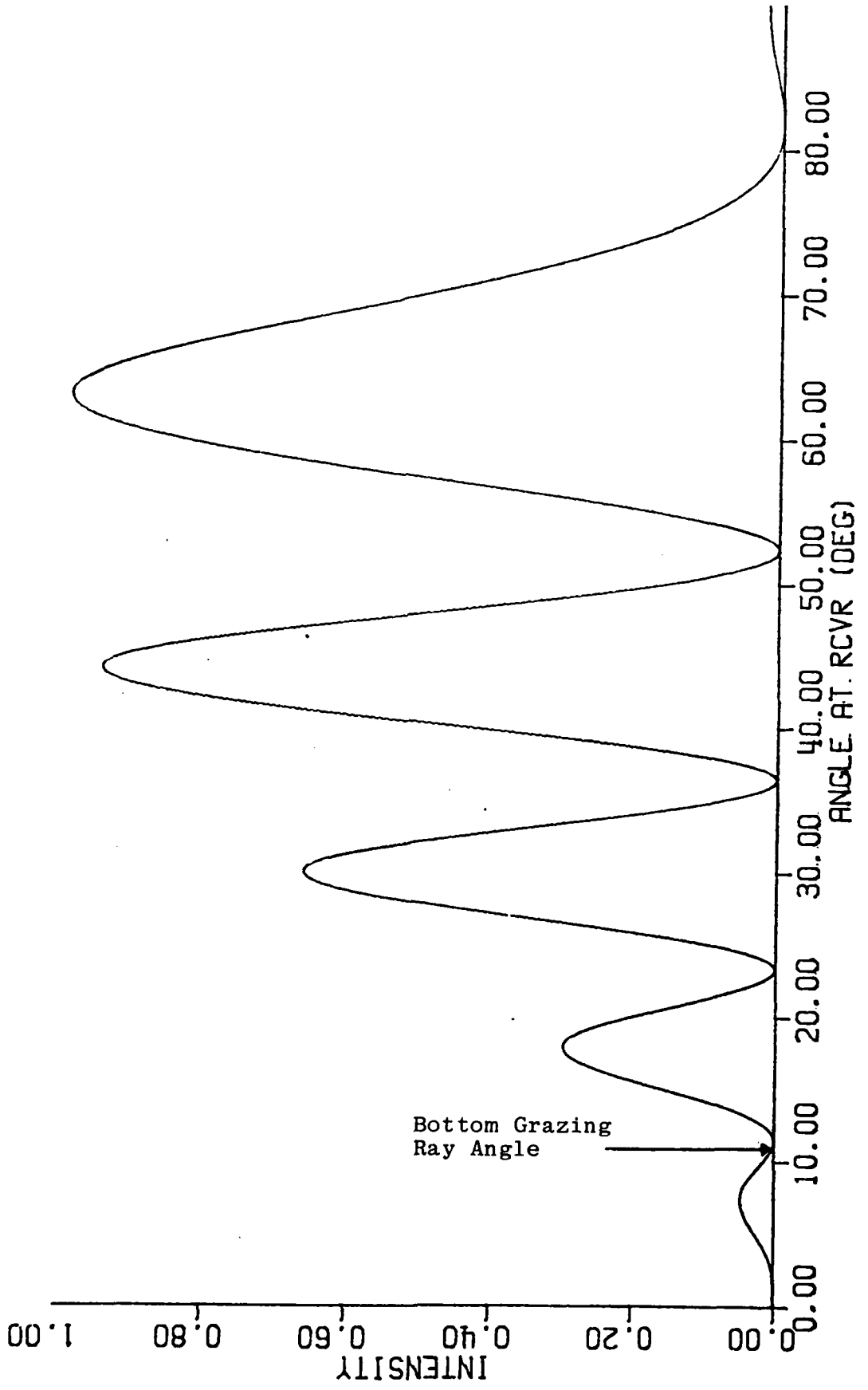

Figure 4-6

Image Interference Function

the "most likely" (in a sense, ensembled over range) fluctuation period would be the one corresponding to the interference generated by angles near the peaks at 17.5° and 30°. The period is

$$\rho = \frac{\lambda}{\cos 17.5^{\circ} - \cos 30^{\circ}} \approx 0.38 \text{ nm},$$

as predicted (Figure 4-4).

Now as the range increases, the arrival angle separation decreases. Hence not only do the arrivals on the peak at 30° suffer greater bottom loss but also it becomes increasingly likely that there are two arrivals high enough up on the peak at 17.5° to matter. In that case, the period of the fluctuations is determined by arrivals at approximately 15° and 20°, i.e.

$$\rho = \frac{\lambda}{\cos 15^{\circ} - \cos 20^{\circ}} = 1.25 \text{ nm},$$

and these periods increase in range as the separation decreases. Again, this is evident in Figure 4-4.

The other parameter of interest, variance, is equally dependent upon the path intensities I_m modulated by the SII effects of Figure 4-6. Recall that

$$\sigma_{\delta I}^2 = 1 - \frac{\sum_{m=1}^{M} I_m^2}{\left(\sum_{m=1}^{M} I_M\right)^2} .$$

If the I_m's are all equal, then

$$\sigma^2 = 1 - \frac{1}{M},$$

ranging from 0.0 for one order and 0.5 for two to 1.0 for large M. As noted above, at the shorter ranges there are two nearly equal orders near 17.5° and 30°, local maxima for Figure 4-6. Furthermore, as the range increases somewhat there are two nearly equal orders for the peak at 17.5°. But as the angle separation decreases still further, additional arrivals have angles approaching 17.5°. Thus, σ^2 is approximately 0.5 at short range and increases beyond 50 nm as additional orders become important.

Particularly interesting is the 30-60 nm range interval, where the fluctuation period jumps several times between values near 0.4 nm (caused by two dominant arrivals near different local maxima of Figure 4-6) and values at or above 1.2 nm (caused by two dominant arrivals near the same local maximum). As will be discussed further, such jumps occur over greater ranges whenever coalescing of two arrival angles near the same peak is impeded (say, for example, if the peaks are narrower).

4.4.2 Observations About Model Sensitivity for the Special Case

With the above discussion of the SII effect in mind, the sensitivity of the fluctuation model predictions to variations in certain of the parameters can be explained.

- Frequency - As the frequency increases (decreases) the peaks on the SII-curve become narrower (wider) and closer together (further apart). Thus, at a higher frequency, say 55 Hz, the first peaks beyond the bottom grazing angle are at 13.1° and 18.4°. Hence at short ranges

$$\rho \simeq \frac{\lambda}{\cos 13.1^{\circ} - \cos 18.4^{\circ}} \equiv 0.60$$

(Note: There is also the effect of scaling implicit in the wavelength). Additionally since the peaks are narrower, it takes longer (in the range sense) for two or more paths to arrive near the same peak. Figures 4-7 and 4-8 verify that the increases in ρ and σ^2 with range are more gradual.

- Source/Receiver Depth - Since source and receiver are interchangeable here, suppose the receiver is shallower. In that case, the SII function consists of the product of two sinusoids: the one with faster oscillations is controlled by the source; it is modulated by a sinusoid with slower variations for the shallower receiver depth. As long as the change in depth does not change the bottom-limiting property, model predictions of ρ and σ^2 are relatively insensitive to changes in receiver depth. However, as the deeper source varies in depth, the location and width of peaks in the SII plot change, much the same as for a frequency shift (the deeper the source, the more rapid the interference).

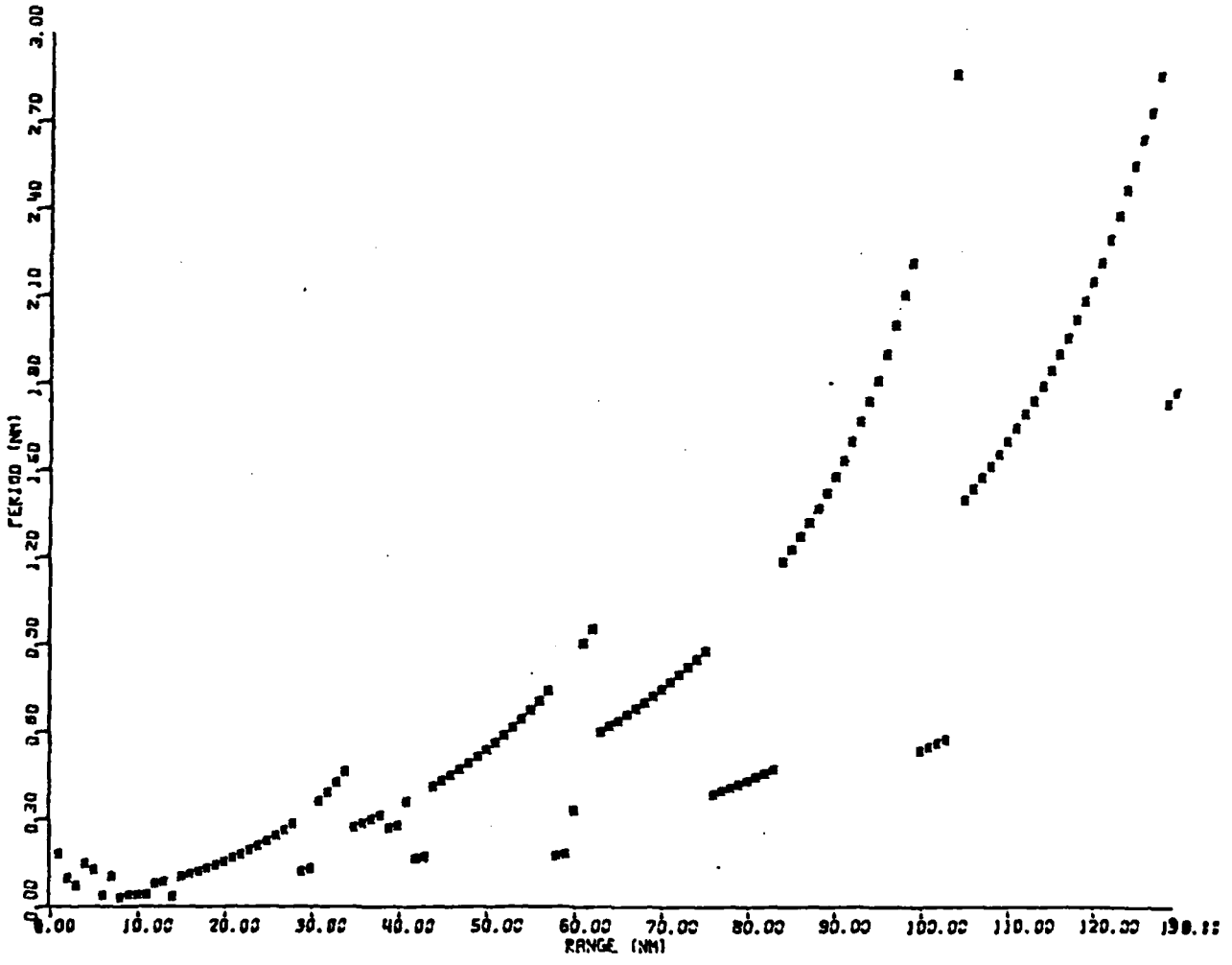

Figure 4-7
Range Period (Same Case as Figure 4-4, but at 55 Hz)

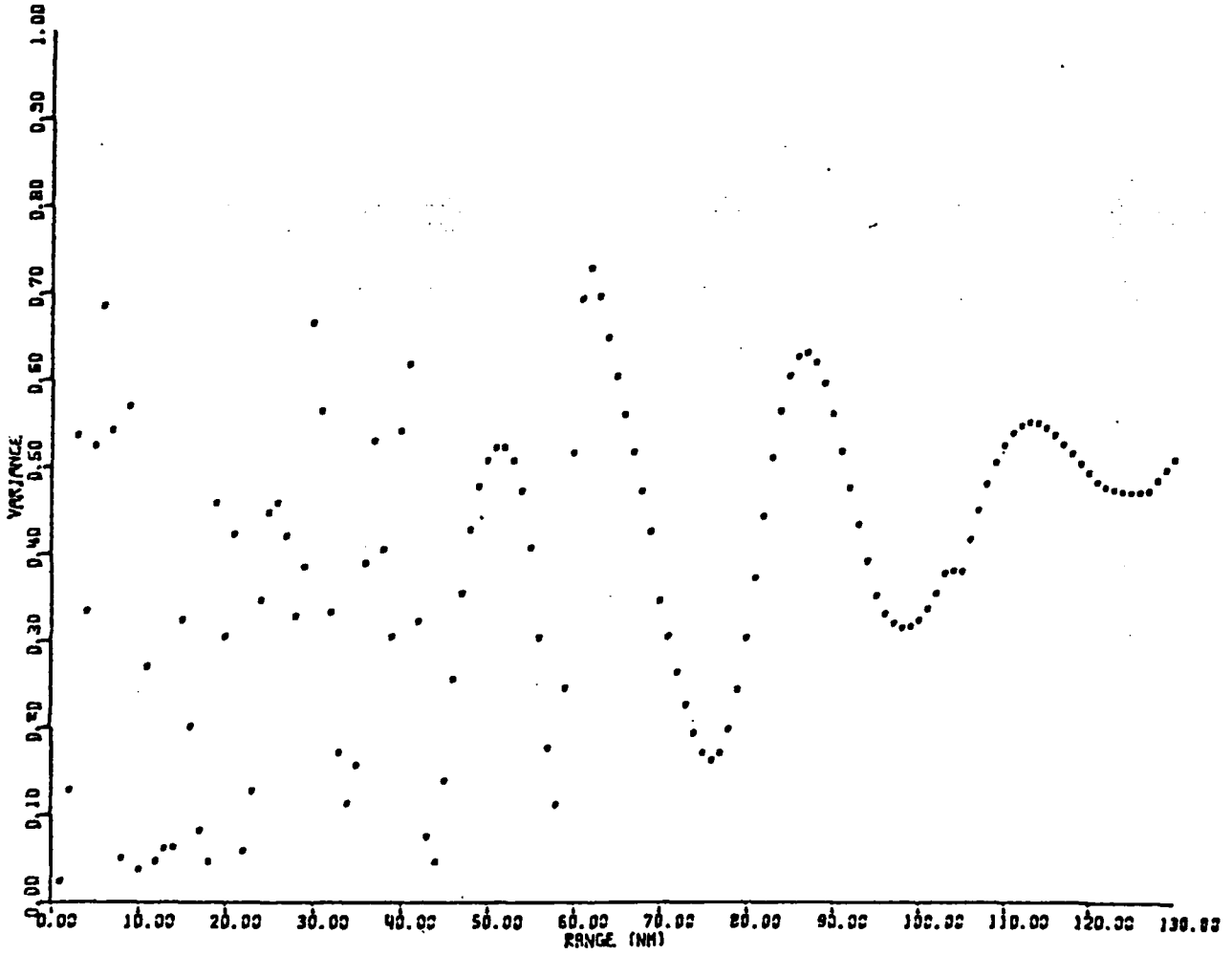

Figure 4-8
Variance (Same Case as Figure 4-5, but at 55 Hz)

Figure 4-9 and 4-10, compared with 4-4 and 4-5, show the small effect of changes in receiver depth from 60 feet to 150 feet, while Figure 4-11 and 4-12 show the substantial changes in ρ and σ^2 when the source depth moves from 500 to 650 feet. In the latter case, the periods jump because dominant-arrivals first appear at angles corresponding to the same peaks in the SII curve, then at different peaks, then back to the same peak again.

To this point all of the examples have been similar because the angle at the receiver that grazes the bottom corresponds to a local minimum in the SII plot. A small change in any of the inputs can cause that angle to occur near a local maximum instead. Then the first peak beyond the grazing angle is effectively only half as large. The net effect is much the same as that of increasing the receiver depth; namely it takes longer (in range) to encounter two arrivals with angles corresponding to that first peak. As an example, consider a case identical to that of Figure 4-9 and 4-10, except that the bottom grazing angle has increased from 10.7^{o} to 12.5^{o} because the bottom sound speed is increased by 30 ft./sec. The resulting model predictions for period and variance are shown in Figures 4-11 and 4-12. Notice that the periods tend to be clustered about the lower values of ρ.

Model sensitivity to sound-speed profile and bottom-loss function is not quite as straightforward as that for frequency and source/receiver depth. A discussion follows.

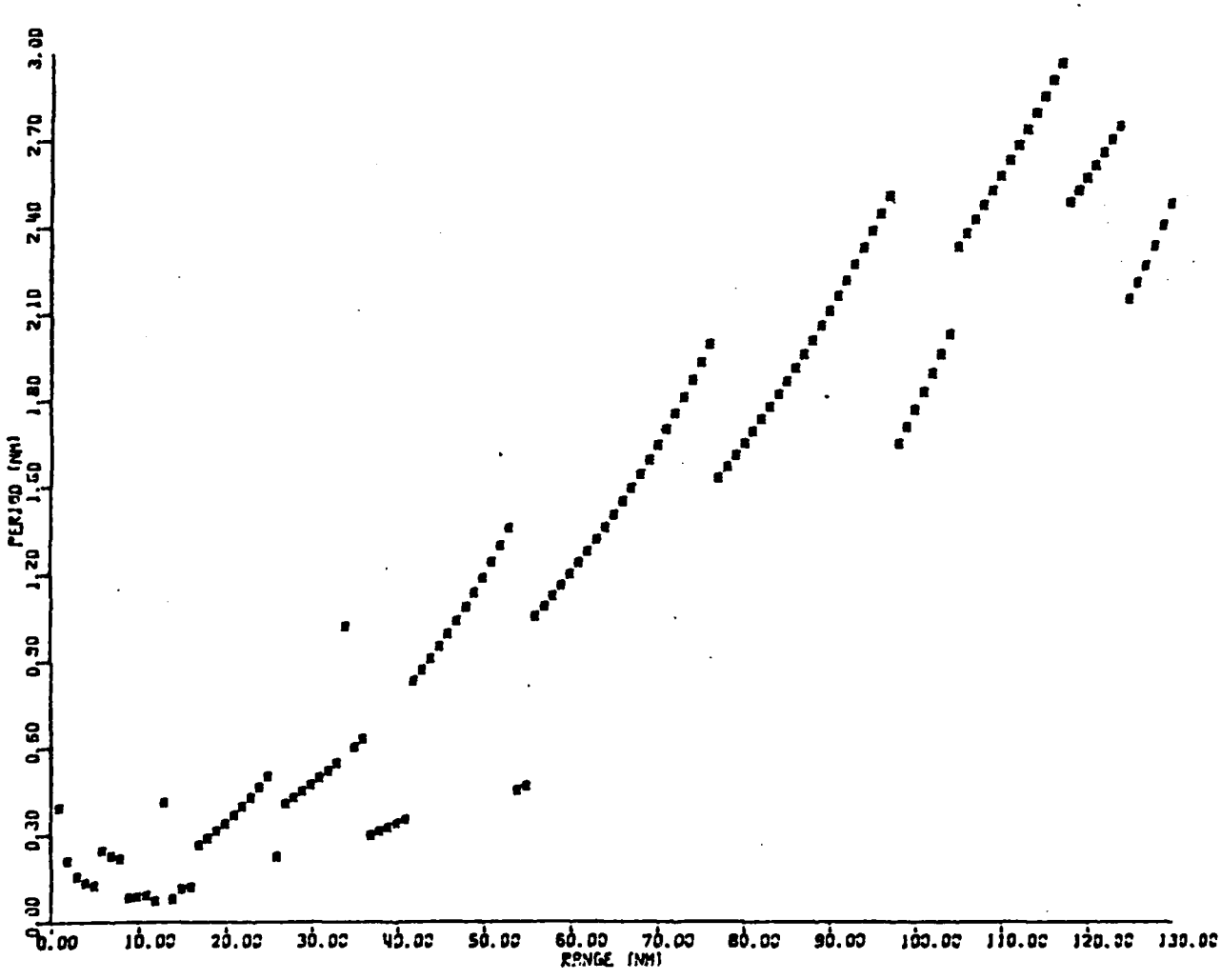

Figure 4-9
Range Period (Same as Figure 4-4, but Receiver Depth = 150 feet)

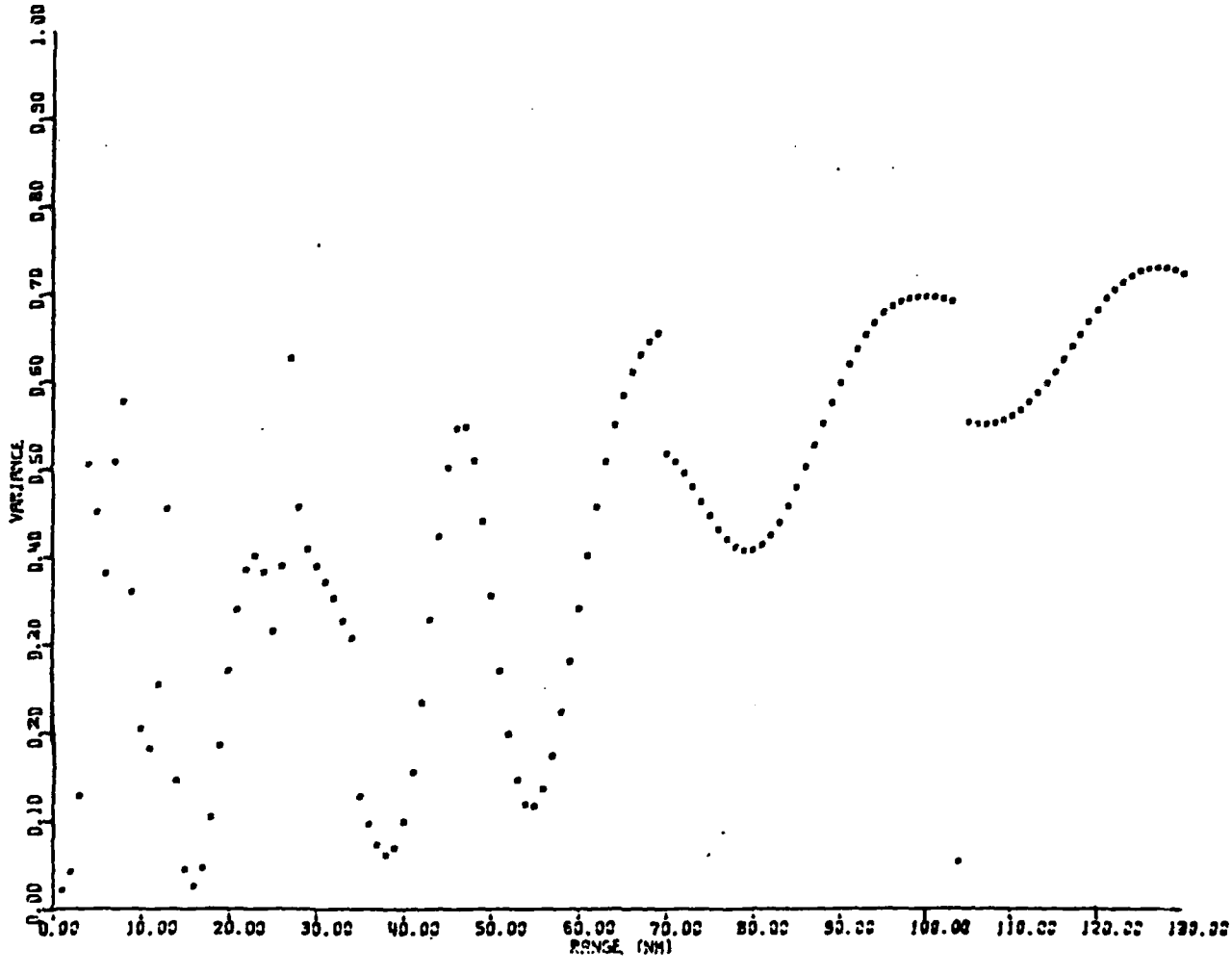

Figure 4-10
Variance (Same as Figure 4-5, but Receiver Depth = 150 feet)

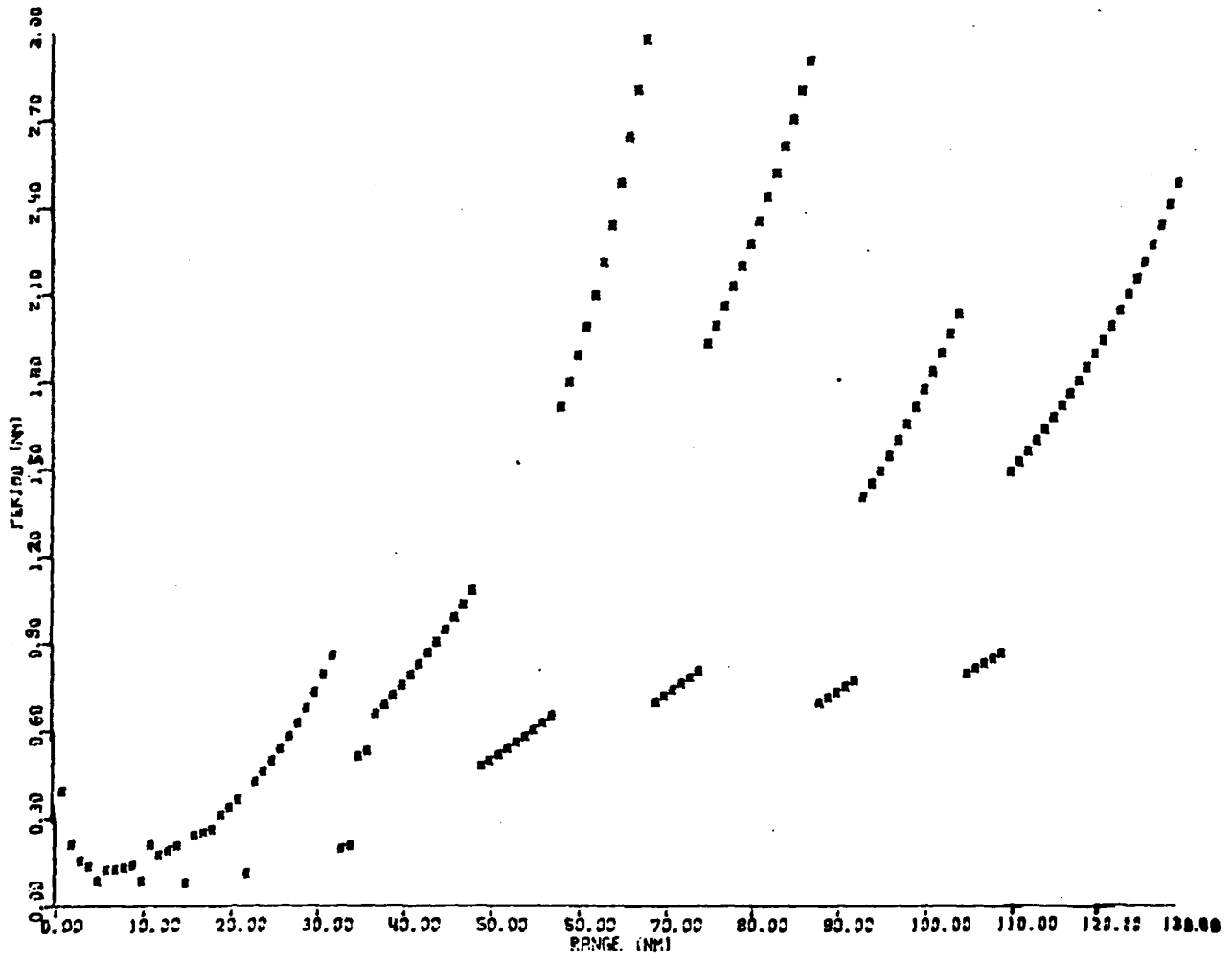

Figure 4-11
(Same as Figure 4-4, but source depth is 650 feet)

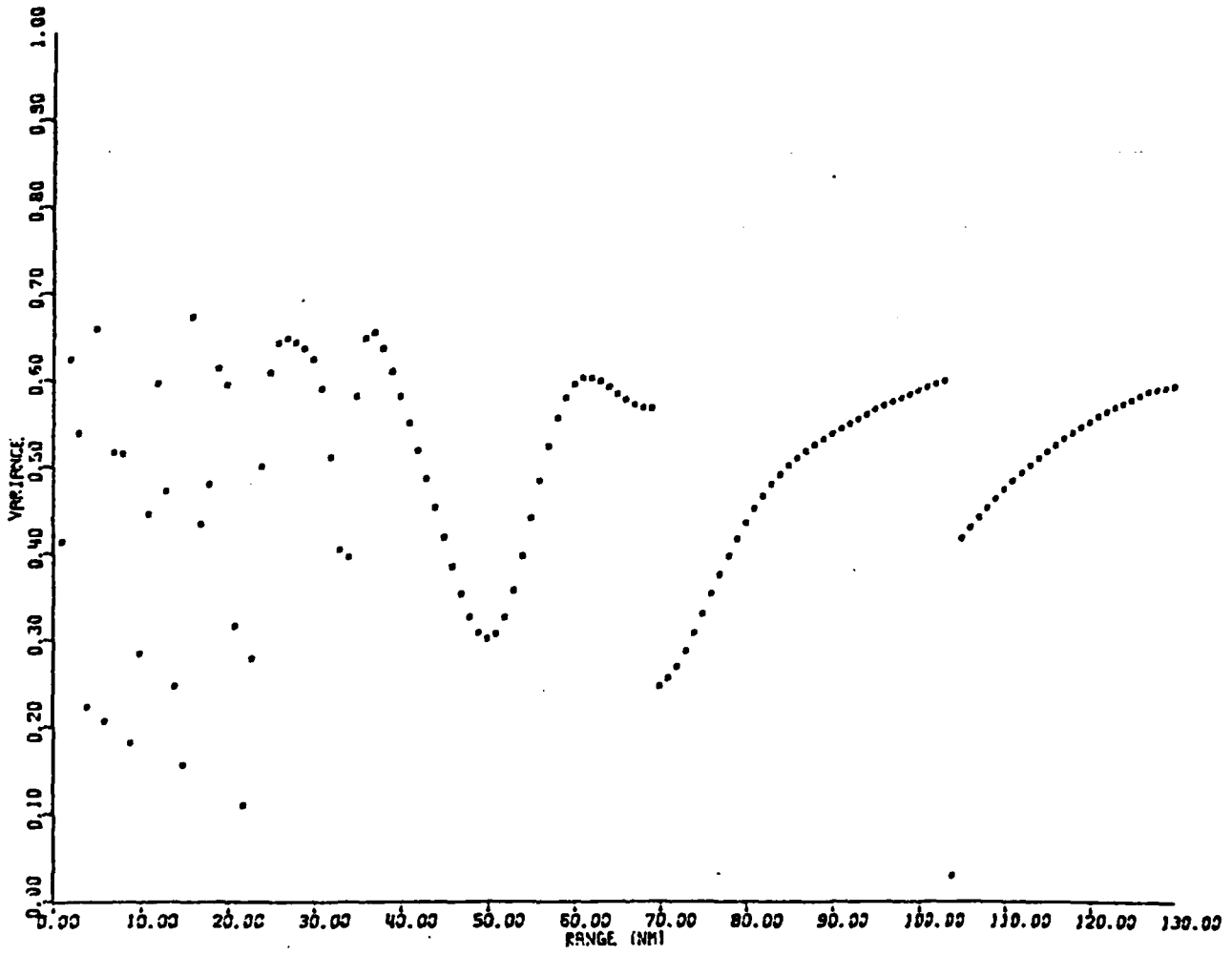

Figure 4-12
(Same as Figure 4-5, but source depth is 650 feet)

- Bottom Loss Function. For bottom loss functions that are independent of grazing angle, results similar to those of the examples discussed thus far can be expected. The only appreciable difference is that the higher order arrivals become increasingly important as bottom loss decreases; in that case the interference generated by arrivals near different maxima in the SII curve is significant to longer ranges.

Bottom loss functions that are dependent upon angle are more complicated. For the important case of low-loss bottoms where paths with grazing angles to 15° or 20° suffer minimal loss,. the computed values of ρ tend to vary more rapidly because there are more arrival orders that have not been attenuated by the bottom.

- Sound Speed Profile. Three distinct sound-speed profiles were selected for comparison:

  - constant-speed profile

  - the Pacific profile described earlier in this subsection, and

  - a pressure gradient profile.

Although not a general sampling, these three do cover a range of conditions and allow certain general statements to be made.

Changes in the profile should affect the model output in two ways:

- A shift of all angles at the receiver and most importantly the angle that grazes the bottom,
- A rescaling of the ray periods for the paths with the shallow angles (the ones of most interest).

The second shift simply changes the rate at which the arrival angle separation decreases with range. The first effect tends to be more important: the bottom grazing angle can be shifted with respect to the maxima and minima of the SII curve resulting in changes in ρ and σ^2 as described above. In addition, a significant change in the environment can introduce a new maximum in the SII curve (on the positive side of the bottom grazing angle) causing substantial variations in ρ and σ^2. As an example, compare Figure 4-13 and 4-14 for the isospeed case with Figure 4-11 and 4-12 for the Pacific profile.

A study of the results for the three profiles has led to a somewhat general way to view the fluctuation models' predictions of ρ and σ^2 for bottom-bounce paths.

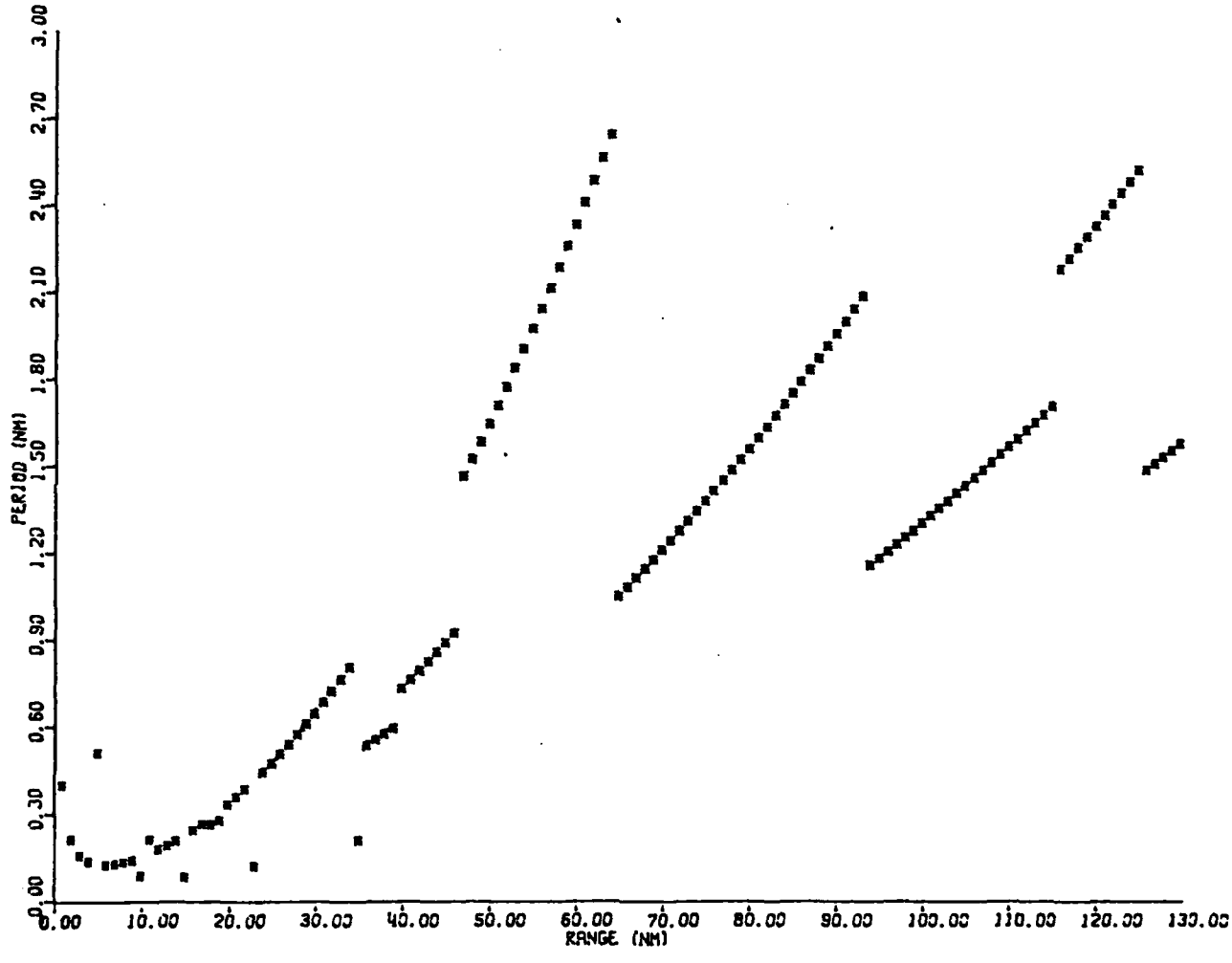
PERIOD (NM)
0.00
0.30
0.60
0.90
1.20
1.50
1.80
2.10
2.40
2.70
3.00
0.00
10.00
20.00
30.00
40.00
50.00
60.00
70.00
80.00
90.00
100.00
110.00
120.00
130.00
RANGE (NM)

Figure 4-13

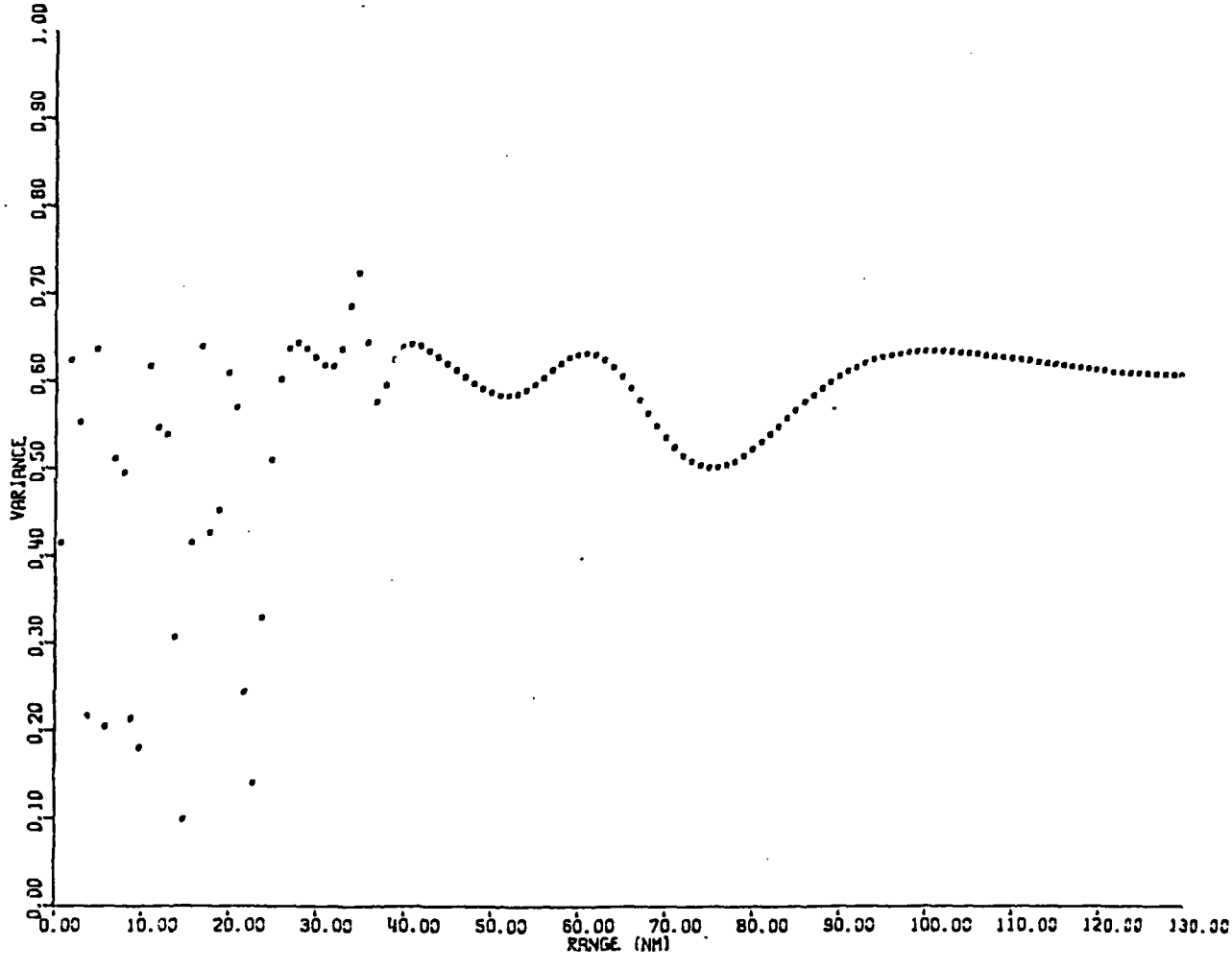
VARIANCE
0.00
0.10
0.20
0.30
0.40
0.50
0.60
0.70
0.80
0.90
1.00
0.00
10.00
20.00
30.00
40.00
50.00
60.00
70.00
80.00
90.00
100.00
110.00
120.00
130.00
RANGE (NM)

Figure 4-14

Consider four range intervals, labeled A, B, C, and D, and the schematics for range-period and variance given in Figures 4-15 and 4-16. Within each range interval there are certain fluctuation properties.

A. Steep-Angle Region. Interference is dominated by interaction of paths with significantly different receiver angles. The range periods, ρ , increases as the first CZ is approached. When SII is important, the variance changes rapidly because of the fast changes in arrival angles with range.

B. Region with Two Separated Orders. Dominant orders have angles near ϕ_1 and ϕ_2 corresponding to the first two peaks of the SII curve, so that period is near

$$\rho_1 = \frac{\lambda}{\cos\phi_1 - \cos\phi_2}$$

When kz_i is large, there may be several important periods, corresponding to other low-angle peaks in the SII curve.

The variance cycles between that for one order (0) and that for two (0.5) as the angles of the orders approach and retreat from the angles of maximum constructive interference in the SII function. B's extent decreases as f and z_i decrease, or as the bottom grazing angle approaches zero.

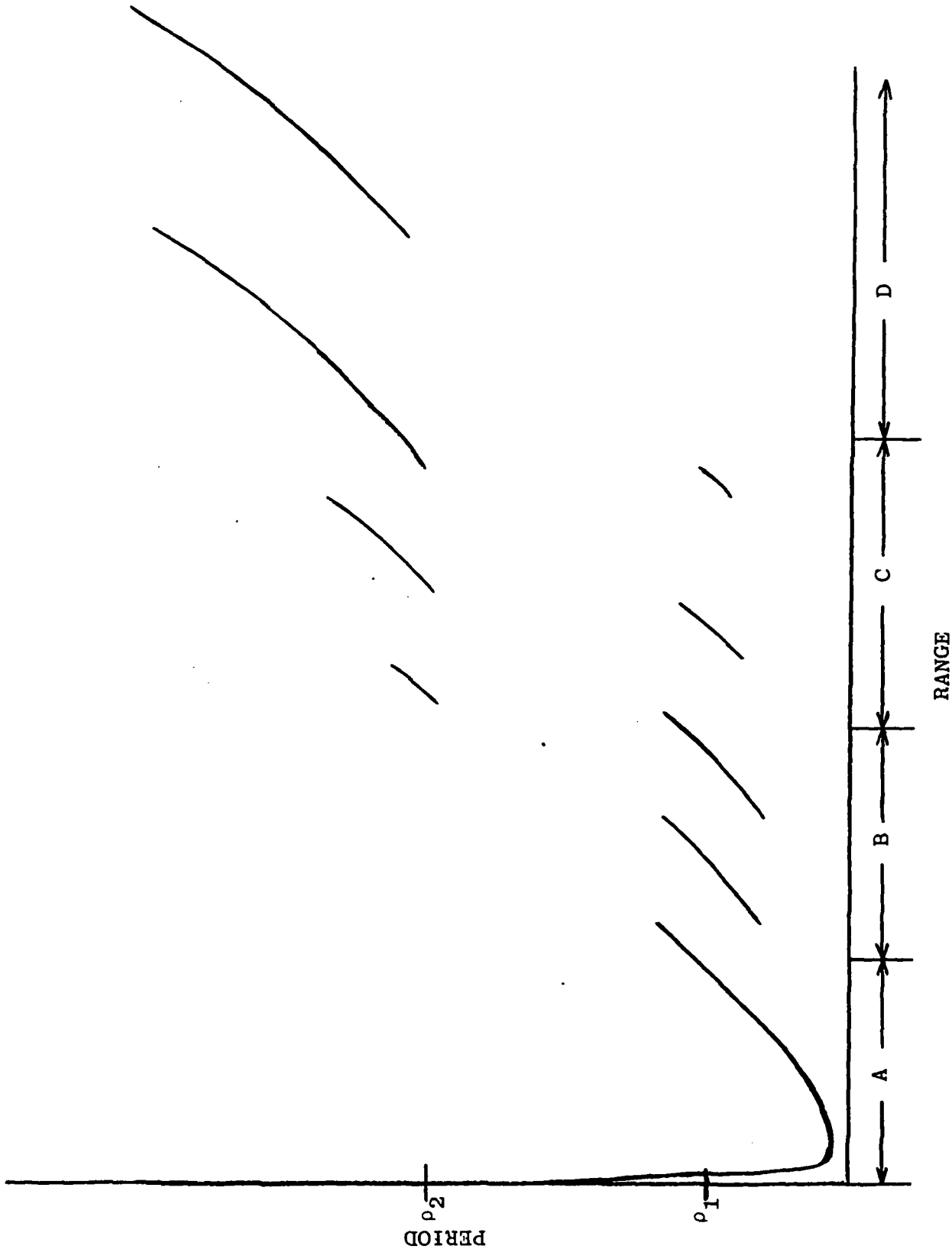

Figure 4-15
General Schematic for Fluctuation Range Periods

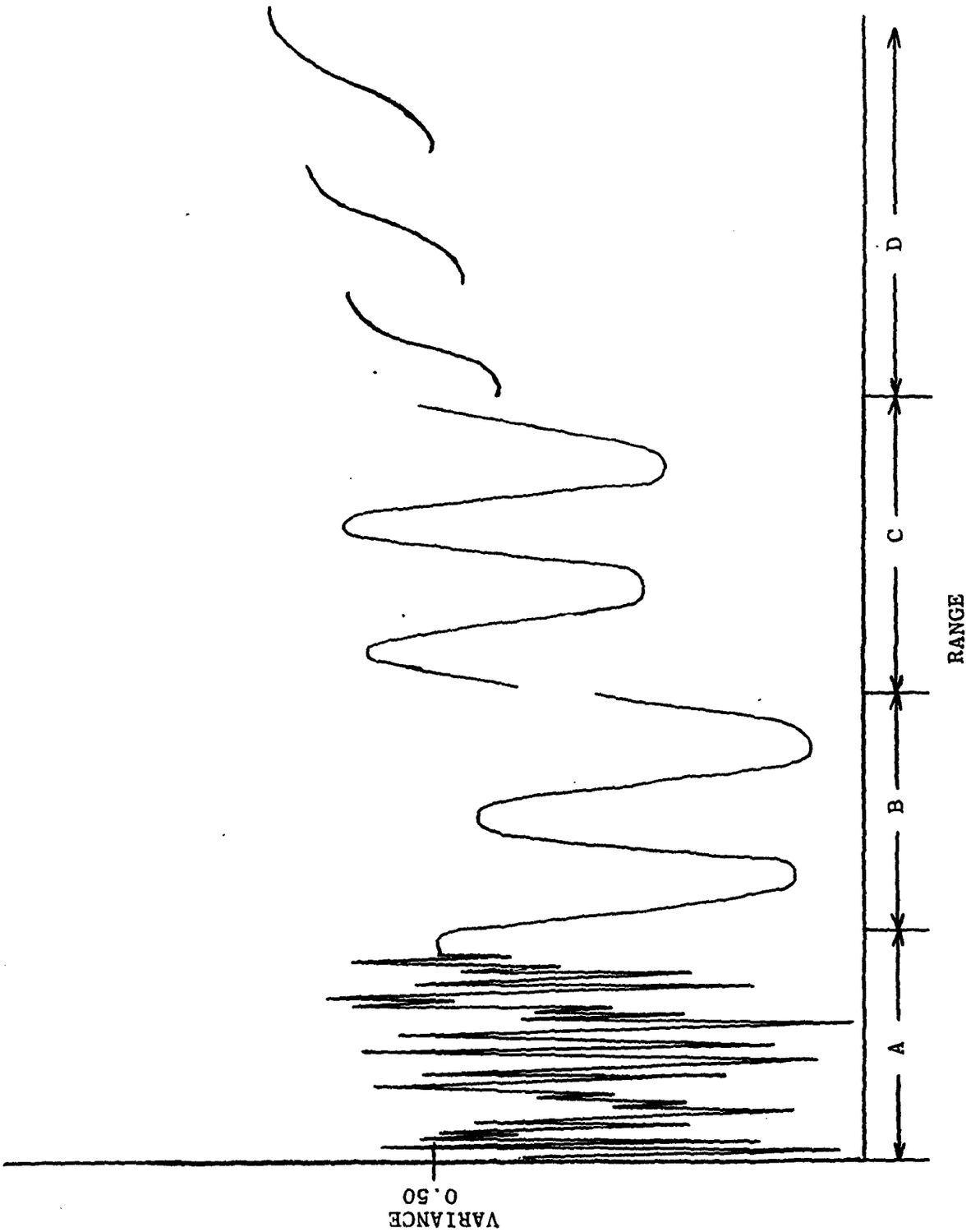

Figure 4-16
General Schematic for Fluctuation Variance

C. Transition Region. Here the important arrivals are both near ϕ_1 or are separated but near ϕ_1 and ϕ_2.

D. Region with Several Dominant Orders With Constructive Interference. Beyond the second CZ (or so), two or more dominant orders have constructive SII near the same angles (ϕ_1). A lower bound on ρ, say ρ_2, corresponds to two paths separated by the width of the interference peak of the SII curve. As range increases more orders approach ϕ_1 and each other, so that ρ increases. Discontinuities are seen as the result of orders "lost" because of destructive interference when the angles go to zero.

The variance begins as that of two orders (0.5), increasing with range as new orders become important, but discontinuously dropping periodically as an order is lost.

SECTION 5
NOISE FLUCTUATION PROPERTIES

A recent report (Ref. 5-1) surveyed models of beam-noise fluctuations. It concentrated on shipping noise and categorized the prediction routines as "Brute Force" (essentially Monte Carlo simulations over source locations, etc...) or "Analytic" (direct evaluation of statistical expressions for input properties of special form). The search for an efficient means to calculate noise fluctuation properties, consistent with the TL approach described above, began with the results of the cited report.

Brute force methods are by definition detailed simulations and hence poor candidates for a short-cut method. Hence, focus was on the Analytic approaches. There are, however, serious questions related to ensembling, as discussed in the report. In particular, "short-term" properties are appropriate for detection models, but differ significantly from the usual output of an Analytic model.

Four Analytic models were considered:

USI	(Ref. 5-2)
Wagner	(Ref. 5-3)
BTL	(Ref. 5-4)
BBN	(Ref. 5-5)

Of these, the USI model was dismissed for several reasons, the most important being the ensembling question, but also because temporal statistics and TL details are not accounted for. The Wagner approach does not apply directly to beam-noise, although certain features were found to be useful,

as discussed below. Of the remaining two, the BTL model was found to be the more advanced, and tests with data had been performed. The BBN model is similar to BTL's. The approach then was to extract from the Wagner and BTL schemes a method for efficiently estimating beam-noise statistics, and then to test the method against Brute-Force simulations from DSBN (Ref. 5-6).

An important modifier for this work are the results of Ref. 5-1 using careful Brute-Force calculations of omni and beam-noise fluctuation properties. There it was found that a "chi-square" model of the distribution and an exponential autocorrelation function were good fits to the data when beam-widths were not too small and nearby ships not overwhelming. Hence, the variance and decorrelation time are the key statistics required. When transient events are important (e.g., single dominated ship), a "nearest-neighbor" approach, such as suggested in the Wagner model, as indicated.

References

1-1. Hanish, S., J. Cybulski, and R. Rollins, "Guidelines for Research in Acoustic Fluctuations" (Workshop results). NESC 320 Report, 1979.

1-2. Cavanagh, R. C., "Acoustic Fluctuation Modeling and System Performance Estimation" (2 Volumes), Science Applications, Inc. (SAI) Report 79-737-WA, 4 January 1978.

1-3. Spofford, C. W., "Acoustic Propagation Modeling of the Effects of Source and/or Receiver Motion," SAI Report, September 1979.

1-4. Cavanagh, R. C., "Review of Models of Beam-Noise Statistics," SAI Report 78-696-WA, November 1977.

2-1. Van Trees, H. L., Detection, Estimation, and Modulation Theory (3 Volumes), Wiley, New York (1968).

2-2. Whalen, A. D., Detection of Signals in Noise, Academic Press, New York (1961).

2-3. Daniel H. Wagner, Associates, "Theory of Cumulative Detection Probaility," Report to U.S.N.U.S.L., 10 November 1964.

2-4. Koopman, B. O., "Probabilities in a Sequence of Correlated Events," OEG Report 59, 29 April 1949.

2-5. McCabe, B. J. and B. Belkin, "A Comparison of Detection Models Used in ASW Operations Analysis," D. H. Wagner Associates Report to ONR (1973).

2-6. Mollegen, A. T., "Review and Comparison of Step Model and Gaussian-Markov Model," op. cit. (Ref. D-8) DTNSRDC, Carderock, MD (1975).

2-7. Belkin, B., "Analytical Results for the Step Process and Gauss-Markov Process in Passive Detection Problems," op. cit. (Ref. D-8) DTNSRDC, Carderock, MD (1975).

References (Continued)

4-1. Cavanagh (Ref. 1-2).

4-2. Dyer, I., "Fluctuations Due to Range Rate," in NRL Memo Report 3884 (Acoustic Fluctuation Workshop) July 1979.

4-3. Clark, J. G., R. P. Flanagan, and N. L. Weinberg, "Multipath Acoustic Propagation with a Moving Source in a Bounded Deep Ocean Channel," J. Acous. Soc. Am. 60, 1274-1284 (1976).

4-4. NRL Workshop (see Ref. 4-2).

4-5. Mediterranean ASW Augmentation Program, Task V, NRL Report 1975.

4-6. Guthrie, K. M., et al, "Long-Range Low-Frequency CW Propagation in the Deep Ocean: Antigua-Newfoundland," J. Acous. Soc. Am. 56 (1974).

4-7. Clay, C. S., "Interference of Arrivals in Continuous Wave Transmission Experiments," Meteorology International Inc., Tech Note Four Project M-153 (1968).

4-8. Hawker, K. E., "A Normal Mode Theory of Acoustic Doppler Effects in the Oceanic Waveguide," J. Acous. Soc. Am. 65, 675-681 (1971).

4-9. Neubert, J. A., "The Effect of Doppler on Long-Range Sound Propagation," J. Acous. Soc. Am. 62, 1404 (1977).

4-10. Tindle, C. T., and K. M. Guthrie, "Rays as Interferring Modes in Underwater Acoustics," J. Sound Vib. 34, 291 (1974).

4-11. Guthrie, K. M., and C. T. Tindle, "Ray Effects in the Normal Mode Approach to Underwater Acoustics," J. Sound Vib. 47, 403 (1976).

4-12. Gerlach, A. A., "Motion Induced Coherence Degradation in Passive Systems," IEEE Transactions on Acoustics, Speech and Signal Processing, ASSP-26, 1-15 (1978).

References (Continued)

4-13. Spofford (see Ref. 1-3).

4-14. Spofford, C. W., Unpublished Report to APL/Johns Hopkins University, November 1977.

4-15. Pedersen, M. A., D. F. Gordon and D. White, "Surface Decoupling Effects," International Workshop on Low-Frequency Propagation and Noise, Vol. II, Maury Center Report (1977).

4-16. Spofford, C. W., "The FACT Model (Vol. I)," Maury Center Report 109, ONR, Arlington, VA (1974).

AD-A108 476 IMPROVED APPROACH FOR MODELING ACOUSTIC FLUCTUATIONS 2/2
(U) SCIENCE APPLICATIONS INC MCLEAN VA
R C CAVANAGH ET AL. OCT 79 SAI-80-104-WA
UNCLASSIFIED N00014-78-C-0603 F/G 17/1 NL

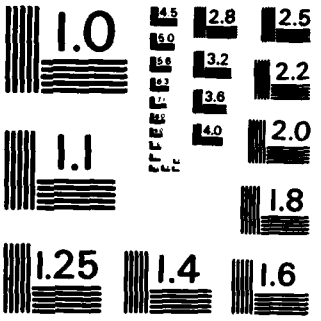

SUPPLEMENTARY

INFORMATION

Errata

AD-A108476

Section 6 is missing and there is no copy available

DTIC - DDAC
120ct83